AN ABSTRACT OF THE THESIS OF

GUY ALAN ARMANTROUT for the M. S. in Electrical Engineering
(Name) (Degree) (Major)

Date thesis is presented June 4, 1964

Title METAL TO GALLIUM ARSENIDE CONTACT EVALUATION USING A VHF BRIDGE TECHNIQUE

Abstract approved [redacted]
(Major professor)

In this paper, the theory of metal-semiconductor contacts was applied to metal contacts on gallium arsenide. A model was discussed which proposed that the contact resistance was due to a highly resistive region between the metal and the semiconductor. In order to evaluate this resistance, a technique using a VHF bridge was developed. In principle, the contact resistance will be shunted at high frequencies due to the capacitances of the resistive region.

A comparison was then made of several different methods of making contact to P-type gallium arsenide. The methods investigated were representative of the methods which are contained in the current literature. The results were statistically analyzed and indicated that alloyed contacts are generally superior to plated contacts. A zinc contact on an etched surface formed the best alloyed contact and a silver contact on a lapped surface formed the best plated contact. Experimental evidence was found to support the proposed model for the contact resistance.

METAL-TO-GALLIUM ARSENIDE CONTACT EVALUATION USING A VHF BRIDGE TECHNIQUE

by

GUY ALAN ARMANTROUT

A THESIS

submitted to

OREGON STATE UNIVERSITY

in partial fulfillment of
the requirements for the
degree of

MASTER OF SCIENCE

August 1964

APPROVED:

[redacted]

Assistant Professor of Electrical Engineering

In Charge of Major

[redacted]

Head of Department of Electrical Engineering

[redacted]

Dean of Graduate School

Date thesis is presented June 4, 1964

Typed by Lucinda Nyberg

ACKNOWLEDGEMENTS

I would like to thank Professor J. C. Looney of the electrical engineering department for his help in the preparation of this paper.

I would also like to thank Tektronix, Incorporated, for the materials used and for their very helpful assistance during this project.

Finally, I would like to thank my wife Arlene for her help and encouragement in completing this study.

TABLE OF CONTENTS

LIST OF FIGURES

LIST OF TABLES

METAL TO GALLIUM ARSENIDE CONTACT EVALUATION USING A VHF BRIDGE TECHNIQUE

INTRODUCTION

Metal-to-semiconductor contacts are an indispensable part of semiconductor device technology since means must be provided for the passage of current between the semiconductor device and the rest of the circuitry. Ideally, the contact should have no effect on the device or circuit operation. It should merely be a transition region of zero resistance — yet at the same time isolate the bulk semiconductor from the effects of minority-carrier injection from the metal. Any resistance in the contact will represent a loss and will degrade the device performance. Likewise, a non-linear low-resistance contact will be a considerable source of distortion in the circuit.

Obviously, it would be desirable to use a contact which has the best properties possible. In order to select the optimum contact, a quantitative comparison needs to be made on the different methods of making contacts. Several different measurement techniques have been developed which are quite satisfactory for germanium, silicon, and low-resistivity gallium arsenide. However, high-resistivity gallium arsenide presents some special problems — both in making contacts and in evaluating these contacts.

It is the purpose of this paper to develop a method of evaluating

the contact resistivity of high-resistivity gallium arsenide. To show the applicability of this method, a series of measurements were made on several representative methods of making contact to P-type gallium arsenide. A statistical investigation of the results allowed reaching the desired conclusions about the contacts. In addition, the measurement method yielded information which was valuable in verifying the model proposed by Hunter's theory of ohmic contacts (14, pt. 3, p. 14).

METAL-SEMICONDUCTOR CONTACTS

Non-ohmic Contacts

Before any semiconductor device can be used, it must be electrically connected to the external circuitry. The easiest method of accomplishing this is by the use of a metal contact.

In a semiconductor, conduction takes place either by free electrons or holes depending upon the material type. Figure 1 shows the energy-band configuration of a typical semiconductor.

The Fermi level, which is an indication of the electron distribution within the semiconductor, is within the forbidden gap. The position of the Fermi level in the semiconductor depends on several factors including the doping of the semiconductor. In the case of N-type material, the Fermi level is closer to the conduction band, and, in P-type material, it is closer to the valence band.

When a metal, which may have a different Fermi level, is brought into electrical contact with a block of semiconductor, charge must be transferred between the semiconductor and the metal such that the two Fermi levels are brought to the same level. The difference in the Fermi levels results in a contact potential which is dropped almost entirely across the region of the semiconductor in contact with the metal. Figure 2 shows the situation when a metal with a lower work function is brought into contact with a block of P-type

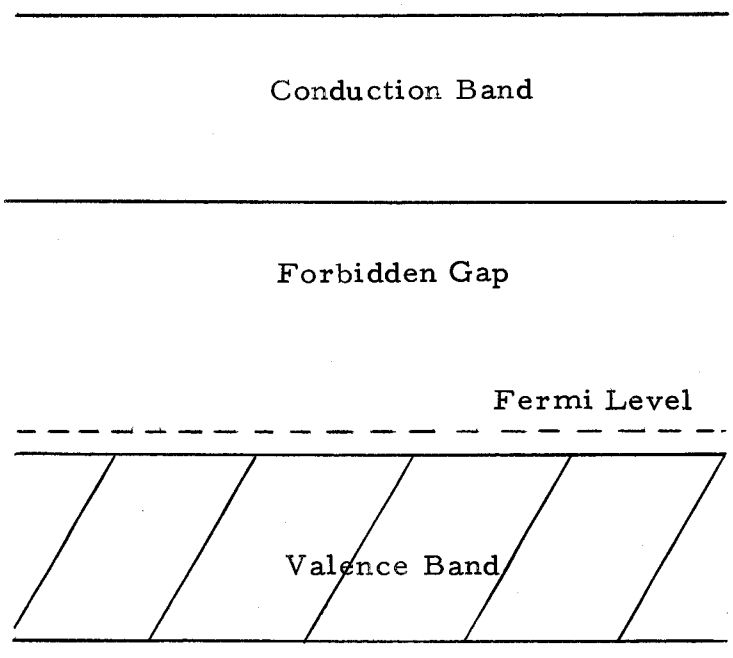

Figure 1. Semiconductor Energy-Band Representation.

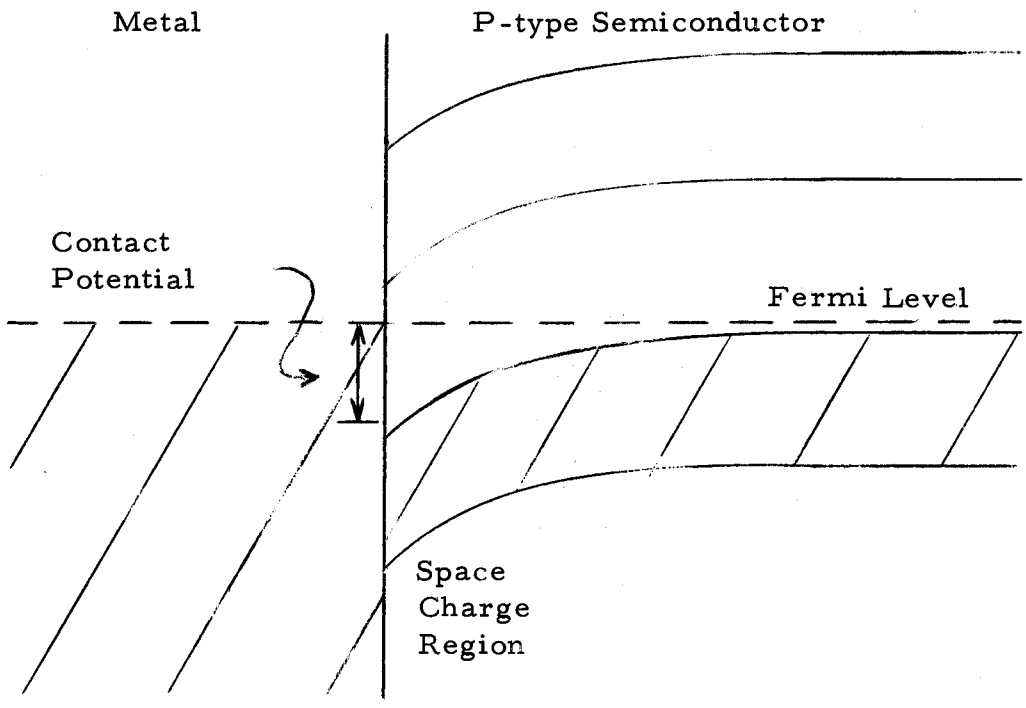

Figure 2. Rectifying Metal-Semiconductor Contact.

semiconductor.

An analogous situation also occurs in the case of an N-type semiconductor when a metal with a higher work function is brought into electrical contact.

In a contact of this nature, it isn't too difficult to see how a non-linear voltage-current relationship results. Referring to Figure 2, assume that a positive voltage is applied to the semiconductor. The net effect is to lower the Fermi level in the semiconductor. This lowers the hole distribution of the valence band such that holes may now easily pass under the barrier resulting in a net current flow.

Now, if a negative voltage is applied to the semiconductor, the effect is to raise the Fermi level and the distribution of holes in the valence band. This reduces the hole flow from the semiconductor to the metal. At the same time, the holes in the metal see a constant barrier and thus current flow doesn't increase with the increasing voltage. Current flow also takes place due to the minority carriers in the semiconductor, but their effect is considered negligible at this time.

The above discussion is based upon the assumption that the relative Fermi levels of the metal and the semiconductor are such that a barrier region is formed between the semiconductor and the metal. The situation also exists where the Fermi levels are such that a potential barrier isn't formed between the metal and the semiconductor.

Figure 3 shows such a possibility where the work function of the metal exceeds that of the semiconductor.

In this particular situation, the holes are transferred from the metal to the semiconductor. A depletion region doesn't exist in this situation as it did in Figure 2. An analysis of the V-I characteristics with the semiconductor biased positively shows that there is no barrier to block hole flow from the semiconductor to the metal and the V-I characteristics should be approximately linear.

If the semiconductor is biased negatively, current and voltage will initially be slightly non-linear due to the small potential gradient extending from the junction into the semiconductor. However, the magnitude of this gradient is usually on the order of 10^{-2} electron-volts and is usually considered negligible. After this, there is nothing to impede the flow of holes and the V-I characteristics are linear. The same reasoning applies to the low-resistance contacts formed on N-type material when the work function of the semiconductor exceeds that of the metal.

The low-resistance contacts just described above are very difficult to attain in actual practice. In the bulk semiconductor, the energy bands are relatively constant except for slight perturbations due to crystal discontinuities and various impurities which determine the material type of the semiconductor. However, at the crystal surface the periodic structure of the crystal is suddenly

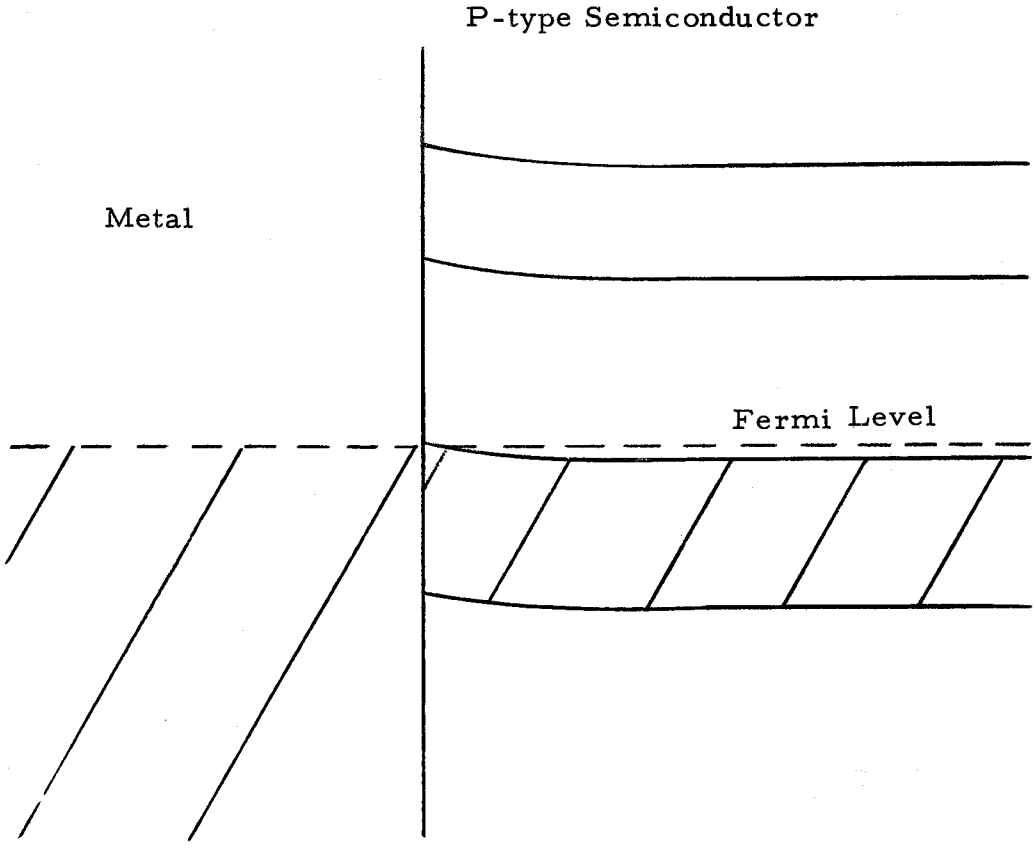

Figure 3. Low-Resistance Metal-Semiconductor Contact.

interrupted. This discontinuity should be expected to shift the energy of the band structure to some different level, which it usually does.

Another problem encountered on the surface of the semiconductor is that of the presence of various impurities. These may be present due to adsorption of various contaminants from etching and washing solutions or directly from the atmosphere. Most of the common semiconductors oxidize to a certain extent when exposed to the atmosphere resulting in another source of surface states. The effect of these surface states may be seen in Figure 4 (11, p. 175;22).

The surface states are fixed in position and act as trapping centers for the majority carriers. Upon acquiring the charged carrier, they shift the position of the band edges such that the Fermi distribution remains constant. In doing so, the energy of the crystal lattice at this point is changed such that similar carriers are repelled resulting in a carrier-depletion region. There are situations where the surface states are sufficiently plentiful at the proper energy level such that an inversion layer exists at the surface of the semiconductor. In the case of Figure 4, this would cause the surface to be N-type while the bulk of the semiconductor remained P-type.

The effect of the surface states has quite an effect on the metal-semiconductor contact shown in Figure 3. Only sufficient charge is transferred in order to equalize the Fermi levels. Bardeen (2) has shown that a surface-state concentration of $10^{13}/cm^2$ is sufficient

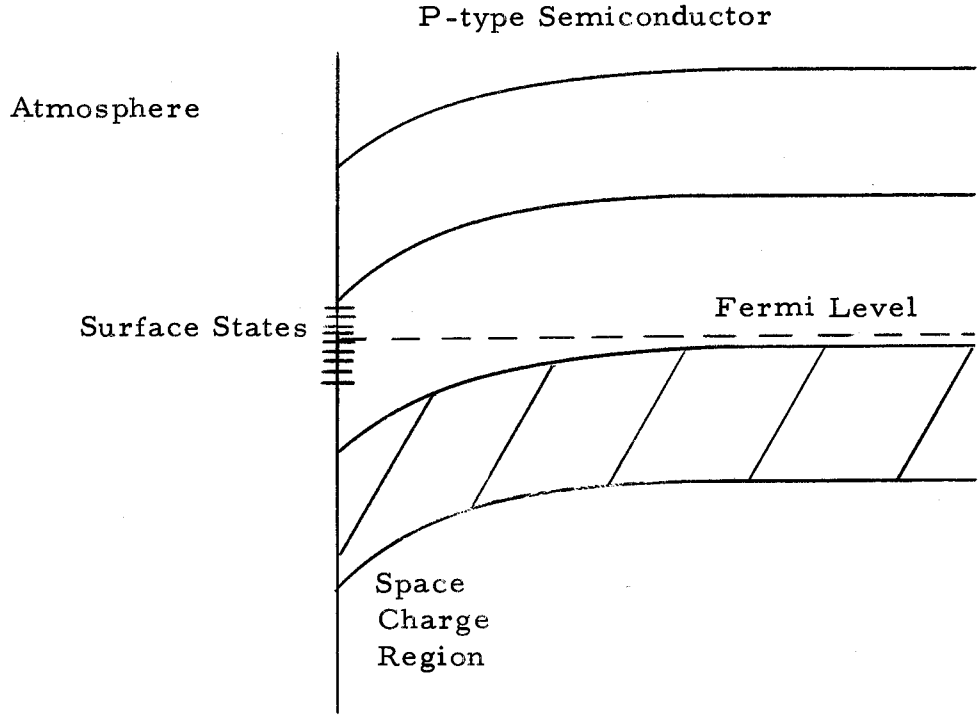

Figure 4. Semiconductor Surface States.

to supply the necessary charge for the alignment of the Fermi levels and at the same time still remains sufficient to maintain the surface states on the semiconductor as shown in Figure 4.

The net result is that a potential barrier now exists in the contact which formerly had a low resistance. The result is similar to the rectifying situation initially discussed and shows that a rectifying contact is formed for practically all non-alloyed metal contacts.

The preceding metal-semiconductor contact theory applies fairly well to gallium arsenide with minor corrections for the larger band-gap and shorter minority-carrier lifetime.

The formation of a potential barrier between a metal contact and gallium arsenide is indicated in all cases due to either the proper difference in Fermi levels or to the existence of surface states which tend to clamp the Fermi level at one point in the bandgap. Spitzer and Mead (30) made a study of the surface states on gallium arsenide. The samples they used were cleaved in a vacuum along the 110 axis and immediately vapor plated with the desired metal. The resulting surfaces should have been relatively free of contamination so that any surface-state indication would be primarily due to the termination of the crystal lattice.

Their results indicated that the Fermi level was tied at a point approximately 0. 6 electron-volts below the conduction band and 0. 8 electron-volts above the valence band. There was very little

dependence of the position of the Fermi level in the forbidden band upon the type of metal plated on the gallium arsenide. Thus, practically any plated-metal contact will result in a rectifying contact on gallium arsenide.

Ohmic Contacts

In the previous section, little attention has been given to the consideration of whether or not a contact is ohmic. The general definition of an ohmic contact is a contact which has a linear voltage-current characteristic and which has no carrier injection from the metal to the semiconductor. The second property is considerably more difficult to measure, but is important since injected minority carriers often greatly affect the bulk properties of the semiconductor. An excellent example is the injection of minority carriers from the emitter into the base of a transistor.

All of the metal-semiconductor contacts previously discussed are non-ohmic to a greater or lesser extent. All of them, including the ideal low-resistance case, are at least slightly non-linear. Likewise, all of them result in a certain amount of minority-carrier injection due to the method of charge transfer across a metal-semiconductor boundary. The injected carriers influence the V-I characteristics to a certain extent by their effect on the bulk resistivity in the region adjacent to the contact. In certain applications,

such as diodes, injecting contacts are quite undesirable.

Methods of Making Ohmic Contact

There are several different methods for making a contact ohmic. The first objective of these methods is to provide a transition between the metal and the bulk semiconductor such that a Schottky barrier isn't formed. As shown earlier, this barrier would impede the flow of carriers across the junction in a non-linear manner. The second objective is to prevent carrier injection by somehow trapping the carriers in the contact region before they have a chance to enter the bulk semiconductor.

One method of achieving these objectives is to mechanically treat the surface so that a continuum of trapping centers is formed in the forbidden band of the semiconductor immediately beneath the surface. These centers are produced when the crystal structure is damaged by any means such as lapping, abrading, or soldering. The effect of these trapping centers may be seen by referring to Figure 5 (14, pt. 3, p. 15). At the surface, the energy band no longer exists as such and a smooth transition is made to the metal. In the semiconductor, the transition to the forbidden gap is gradual and results in the formation of no potential barriers. This contact is ohmic since the V-I characteristics are linear and any minority carriers injected from the metal recombine in the transition region before entering the bulk semiconductor.

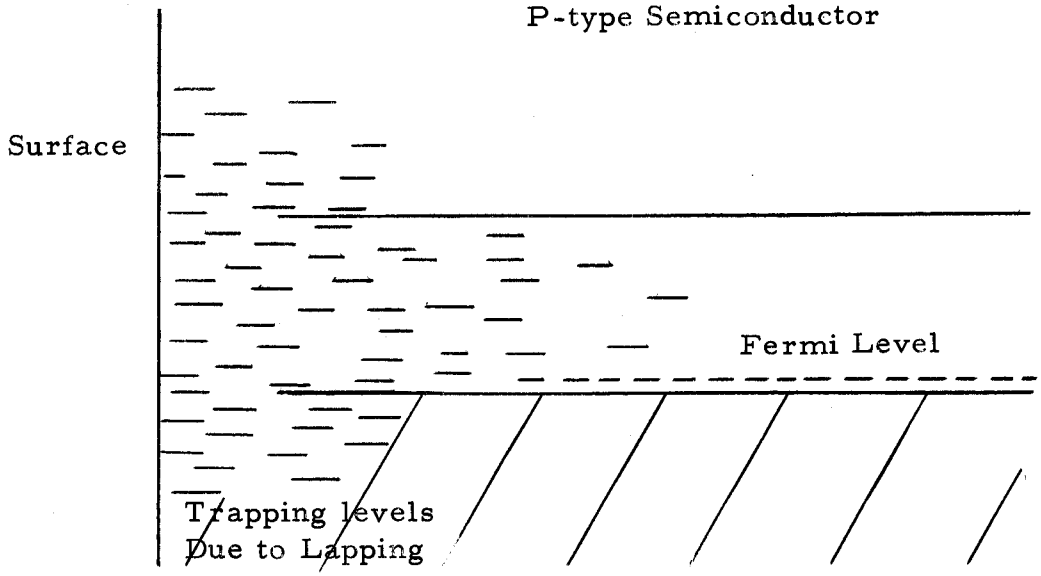

Figure 5. Lapped Semiconductor Surface.

An alternate method of making ohmic contacts, which is commonly used, is to dope the surface of the semiconductor quite heavily such that it begins to take on the characteristics of a metal. Some of the doping impurities will diffuse a short way into the semiconductor and will result in a very heavily doped region of the same type as the bulk material. The transition between this region and the metal is gradual due to the metallic nature of the semiconductor surface and contains no barriers. The transition between the heavily doped and lightly doped regions has also been shown to be ohmic with negligible resistance (29, p. 276).

Model of an Ohmic Contact

The "ideal" theory of ohmic contacts presented above assumes that there is no contact resistance as such, but only the body resistance of the metal and the semiconductor. Hunter presents a more realistic approach by recognizing the presence of a finite resistance at the contact not associated with the individual resistivities (14, pt. 3, p. 14). In the rectifying contacts previously presented, the existence of the barrier required that the thickness of the barrier be negligible compared to the diffusion length of the minority carriers passing through the junction. If this criteria isn't fulfilled, then the barrier region ceases to be a barrier and becomes a region of high resistivity. Thermodynamic equilibrium requires that charge

neutrality conditions be maintained within this region. Under these conditions, it is seen that the charge-depletion region, which is required for a barrier, won't exist and the contact is ohmic. Due to the high-recombination rate, essentially all the minority carriers are trapped and injection is prevented.

This model explains the reasoning behind the methods of making ohmic contact which were previously discussed. In these methods, the main objective was to produce a region which had a very high recombination rate.

The existence of contact resistance is often ignored or considered negligible when viewed from an economic view point. However, its existence is recognized. Nibler has studied the contact resistance of many of the popular methods for making ohmic contacts to germanium and silicon (25). The contacts which he studied had a linear V-I characteristic. He attributed the contact resistance to a thin, semi-insulating layer somewhere between the semiconductor and the metal through which the carriers tunneled. This is similar to the high-resistivity region which Hunter describes. Nibler also found that an apparent correlation exists between the contact resistivity of a metal contact and the bulk resistivity of the semiconductor. His expression for the contact resistivity, ρ_c, was: $\rho_c = A\ \rho^B$ where A = 14, B = 1 for N-type germanium and A = 3.3, B = 1.3 for N-type silicon.

A study done by Texas Instruments, Incorporated, (31) on the contact resistivity to gallium arsenide indicates that an appreciable resistance does exist strictly due to the metal contact even on very low-resistivity material. Research reported later in this paper also indicates the existence of a definite contact resistance which appears to follow Hunter's model of a thin layer of highly resistive material.

CONTACT-RESISTANCE-MEASUREMENT TECHNIQUES

The probable existence of a finite contact resistance has been established. The value of this resistance isn't fixed, but varies a great deal depending upon the material type, doping levels, contacting material, method of making contact, surface cleanliness, and even the technician himself. The problem at the present time is to measure and evaluate the contact resistance. This measurement makes it possible to then compare different methods of making ohmic contact such that the procedure may be optimized to obtain the lowest-resistance contact with the desired properties.

Body-Resistance-Calculation Method

There are several current methods for evaluating the contact resistance in addition to the VHF bridge method used in this presentation. Perhaps the most obvious method is to calculate the body resistance of the specimen. Then the total resistance may be measured and the difference attributed to the contact resistance. This method has the advantage of being quite easy to perform. Also, it provides an easy estimate of the barrier resistance in the case of a rectifying contact where the contact resistance can't be represented by a fixed value of resistance.

There are several problems associated with this method.

First, only the average bulk resistivity is usually known. Any variation in the homogeneity of the sample will result in a body resistance which is considerably different from the calculated value. This will show up as an error in the contact-resistance estimation. When the value of the contact resistance is fairly small compared to the bulk resistance, this method becomes highly impractical. Another complication which often shows up in the case of small-area contacts is that of the spreading resistance. An accurate calculation of this resistance is usually quite difficult due to such things as geometry variation and minority-carrier injection.

Potential-Probe Method

The most widely accepted method at the present time for reasonably accurate contact studies is the use of a potential-probe technique. This method appears to be quite satisfactory for contact studies on silicon, germanium, and low-resistivity gallium arsenide. However, it has several serious limitations which will be discussed later.

This technique is similar to the four-point-probe technique for measuring bulk resistivity. In the potential-probe method (16, p. 58; 31), a current field is established in the sample using the contacts to be investigated. A movable probe is then used to measure the potential along the bar as a function of distance (See Figure 6). As may be readily seen, an initial voltage jump occurs at one of the

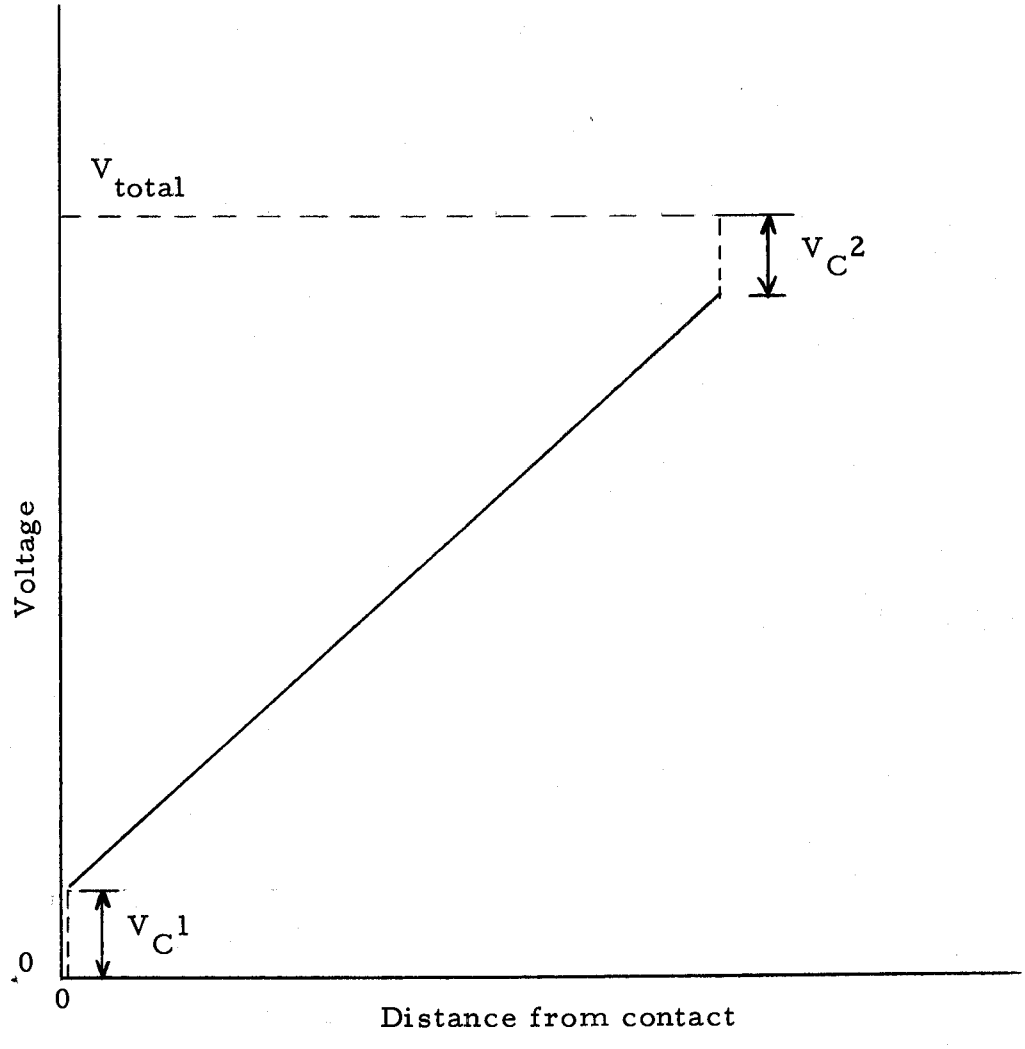

Figure 6. Potential Plot of Moveable-Probe Method.

contacts. Then the gradient along the bar is plotted up to the next contact where another jump occurs. These voltage jumps represent the drop across the contact resistance. If the contacts are ohmic such that the contact resistance doesn't depend on the voltage, then the value of this resistance may be calculated by taking the ratio of the voltage drop to the current passing through the contact.

This method of measuring contact resistance has several distinct advantages over the method previously described. Most important is the fact that this method doesn't depend on the sample homogeneity. The plot which is taken may follow any path and isn't necessarily the straight line shown for a homogeneous sample. The only really important point is the voltage jump which indicates the contact resistance. Of course, proper evaluation at this point requires a sample geometry which doesn't include any potential drops across the semiconductor or the inclusion of a spreading-resistance region in the measurement of the contact drop.

Another advantage is that the characteristics of two separate contacts aren't lumped together. Any slight non-linearity between contacts which are sensitive to the direction of current flow is detectable.

Despite the advantages, there are also several distinct disadvantages. First among these is the problem of accurately determining the position of the potential probe. Highly precise instruments

are required. Any error in position estimation which allows a small portion of the semiconductor gradient to be measured as part of the contact-potential drop increases the apparent contact resistance. Likewise, if an error is made such that the contact drop is considered as part of the sample gradient, then the apparent contact resistance will be too small. An approximate estimate of the accuracy required can be calculated from the contact resistivity measured on low-resistivity P-type gallium arsenide in Texas Instrument's report (31). The sample resistance included as an error should only be about 10% of the contact resistance. The variation in distance which must be known is given by $L = \frac{0.1\ \rho_c}{\rho}$ where ρ_c = the contact resistivity in ohm - cm^2 and ρ is the bulk resistivity in ohm-cm. Substituting the appropriate figures gives L = 0.005 centimeters or about two mils. This accuracy may be difficult to achieve.

Another major problem is the type of contact which is formed by the movable probe. According to the theory covered in section one, this will be a rectifying contact due to the surface states. This effect can be minimized to a certain extent by lapping the surface prior to measurement. Heavily doped material is almost metallic in nature and forms a fairly good ohmic contact with the probe. This was the case in the Texas Instrument study.

The problem of a rectifying contact was discussed by Henisch (11, p. 275) in his studies using a potential-probe technique. One

of the problems which he indicated is the potential which appears across a recifying contact which is sensitive to incident light. A greater problem is due to the pickup of stray signals by the circuit wiring. These are rectified and appear as an undesirable D-C level across the junction causing an error in the measured potential. Henisch indicated a solution to the problem by using formed or alloyed contacts which would make the rectification ratios much smaller. A rectification ration of 2 : 1 was considered satisfactory while a ratio in excess of 4 : 1 was considered too large.

Some of this problem could be overcome by using an A-C or pulse source rather than a D-C source. However, another problem arises in as much as the resistance of the probe on high-resistivity gallium arsenide is essentially infinite for either voltage polarity up to about ten volts. A sample of 0.1 ohm-cm N-type gallium arsenide was checked with one ohmic contact and a tungsten probe. The current indicated a resistance in excess of ten megohms. This isn't unreasonable considering the high resistivity and large bandgap of the material.

This "insulating" property makes potential measurements with this technique extremely difficult if not impossible. An alternative is to form the contacts as suggested earlier. However, this makes position determination quite difficult due to the larger contact area and introduces considerable error.

Even though the potential-probe technique does have several advantages, it is extremely difficult to use in measuring contact resistance on high-resistivity gallium arsenide (About 10^{16} to 10^{17} carriers/cm^3). Also, it doesn't give any information about the model which may be used to explain the contact resistance.

VHF Bridge Method

As an alternative method of contact evaluation, a VHF bridge method was developed and investigated and appears to be quite satisfactory.

The basic principle is quite simple. At some high frequency, any resistance due to the contacts should be effectively shunted by the contact capacitance. A high-frequency technique has been used in the past to measure the conductivity of a powdered sample (16, p. 59). At sufficiently high frequencies the contact resistance between the particles was eliminated allowing accurate measurement of the material.

The effect of the barrier capacitance has been used also to study the contact characteristics of rectifying junctions in selenium rectifiers. In these studies, the impedance of the contact was measured as a function of frequency and plotted on polar coordinate paper. The result allowed a determination of the rectifier capacitance vs. frequency and the value of the body and back-contact resistance

combined. All of these studies were carried out at frequencies from 0 to 100 KC (11, p. 156).

A model may be used to represent the total system of two contacts on a piece of semiconductor as shown in Figure 8. The physical structure of the sample (Figure 7) suggests such a model since the resistance may be split into three parts. A reasonable amount of capacitance is associated with each contact due to the narrow dimensions of the resistive region. It is reasonable to assume that this capacitance would tend to shunt the small contact resistance at some elevated frequency. Henisch has suggested the possibility of such an occurence in his analysis of the selenium rectifiers, but no results were reported (11, p. 156).

The impedance of this circuit as a function of frequence, ω, may be easily derived. Several simplifying assumptions are first made to make the result more usable. First, the stray capacitance is considered negligible due to the relative levels of the resistances in the circuit. The sample holder which was used contained a negligible amount of stray capacitance.

Secondly, assume that the two contact resistances and their associated capacitances are equal. This greatly simplifies the analysis and results in only two significant break-points. The assumption seems fairly reasonable for identical ohmic contacts on the same piece of material. As it turns out, deviations from equality aren't

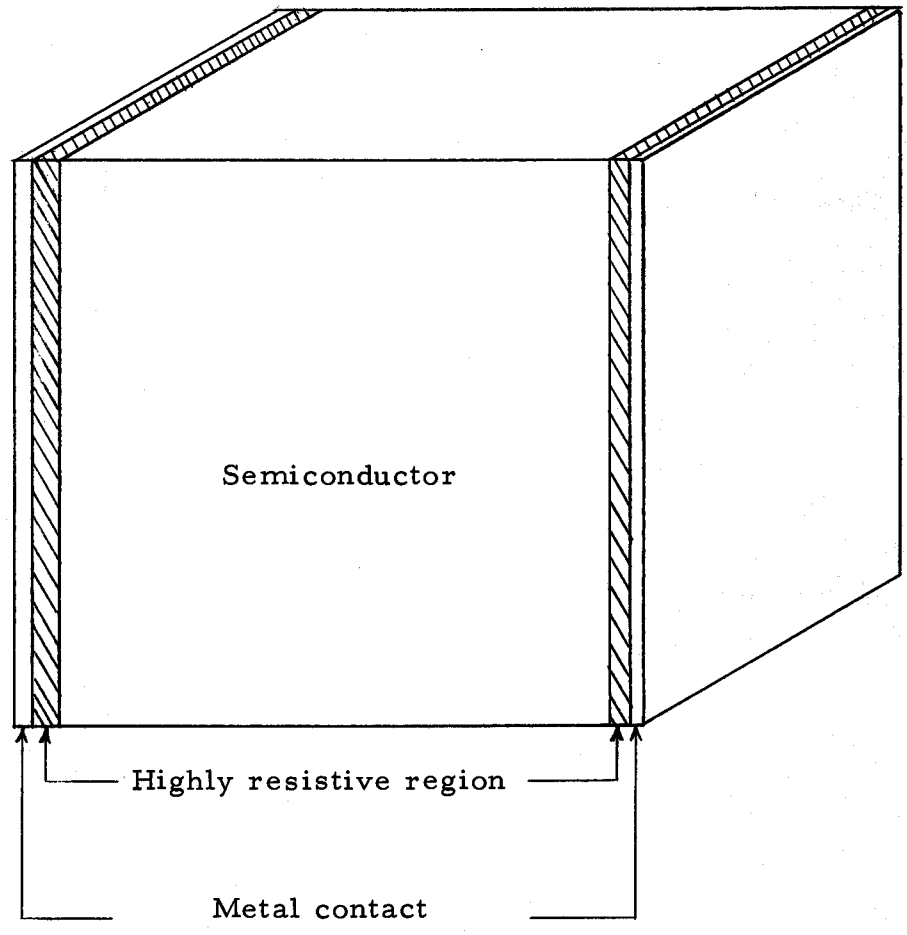

Figure 7. Physical Structure of Semiconductor and Contacts.

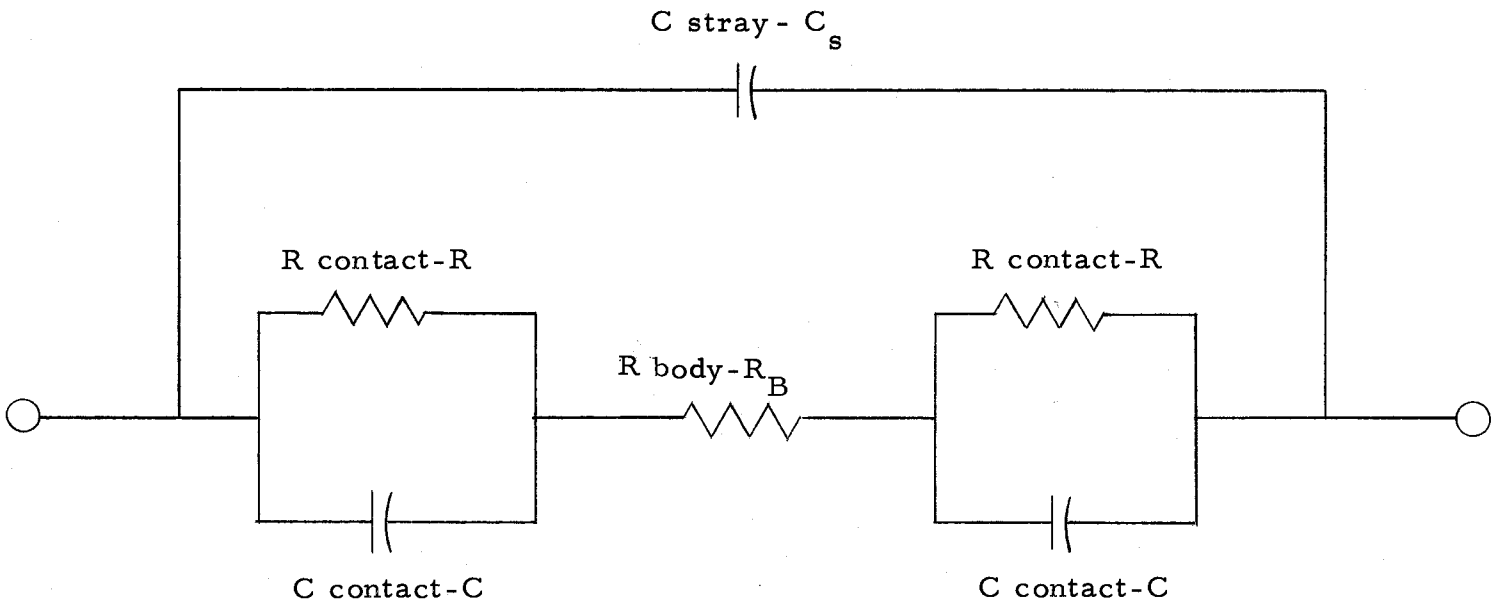

Figure 8. Electrical Equivalent of Figure 7.

too serious. As will be shown later, the RC time constant of this circuit remains essentially constant even with varying contact resistance. Thus, no new break-points will be introduced in the response and the only problem will be a partition of the measured contact resistance between the two contacts. For identical ohmic contacts they are equal.

Under the above simplifying assumptions, the expression for the impedance Z becomes:

$$Z = \frac{R_B R^2 + X_C^2 (2R + R_B)}{R^2 + X_C^2} - j \frac{2X_C R^2}{R^2 + X_C^2}$$

where: R = contact resistance
C = contact capacitance
R_B = body resistance

or, in terms of ω and simplifying:

$$Z = R_B + \frac{2R}{1 + R^2 C^2 \omega^2} - j \frac{2R^2 C\omega}{1 + R^2 C^2 \omega^2}$$

The validity of this expression may be seen by setting $\omega = 0$. At this point, $|Z| = R_B + 2R$. As $\omega \to \infty$ $|Z| \to R_B$. A general plot of $|Z|$ versus ω is shown in Figure 9. In this plot, it can be seen that the total resistance is measured at low frequencies. Then the shunting effect of the contact capacitance is given by the first drop after which the curve levels out again at R_B. At higher frequencies the impedance starts dropping due to the stray capacitance.

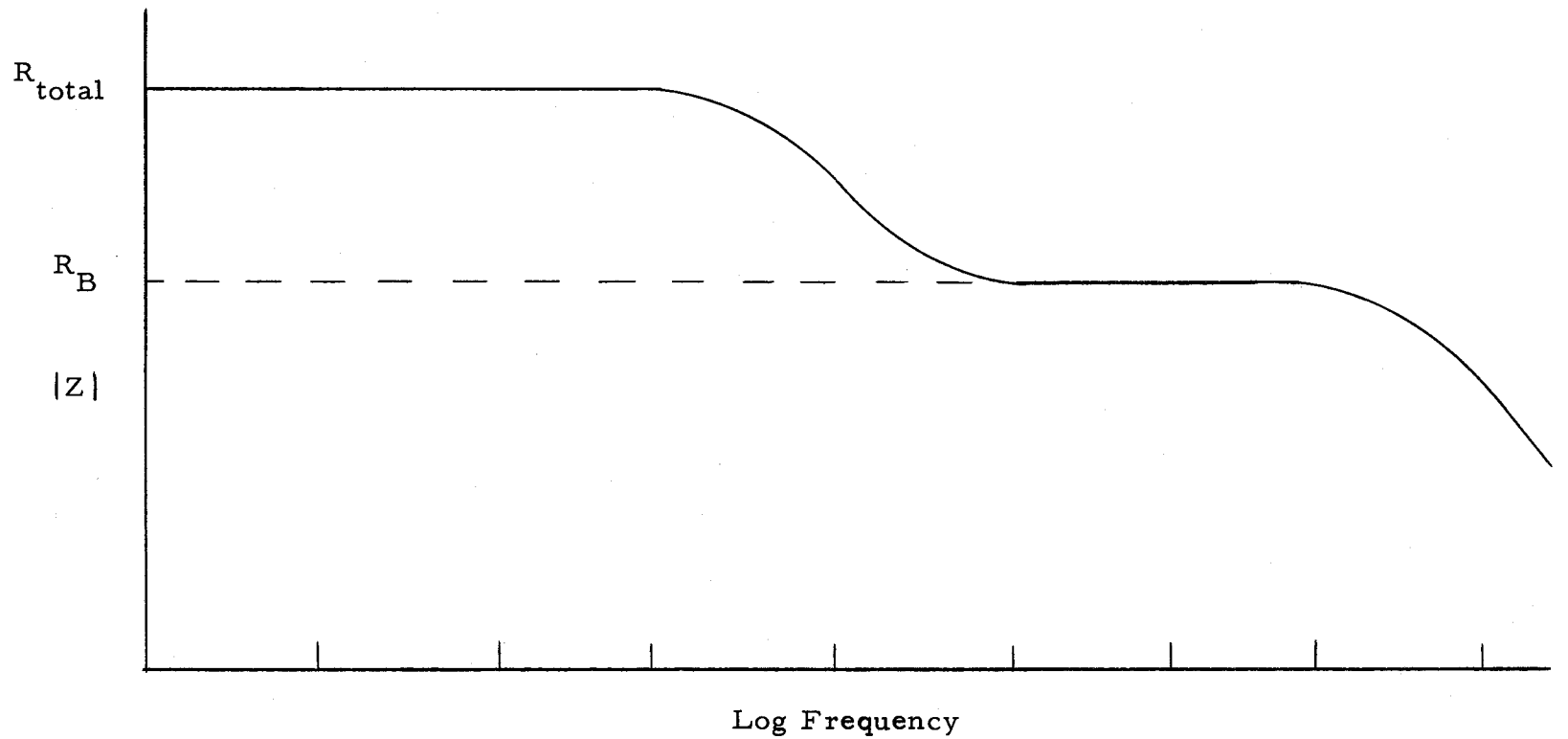

Figure 9. |Z| Versus Frequency.

Application of the VHF Bridge

Of course, the ideal measurement of a sample would include taking the entire frequency response of the sample. Then the various values of resistance could be easily determined. However, this would require quite a few decades and most bridges only cover one or two decades in their operating range.

The above problem may be resolved by the following procedure. A frequency, ω_1, may be defined as the point at which $\omega_1 = 1/RC$. In addition, the total values of resistance may be set equal to one so that a normalized curve may be plotted. It will be noted that Z is a function of both R and R_B. If the value of either one is known and the total resistance is known, then the value of the unknown resistance may be determined. Likewise, if the ratio R/R_B is known along with the total resistance, then both R and R_B may be calculated. A different plot of $|Z|$ will result for each ratio of R/R_B on a normalized scale. A family of curves with R/R_B as the variable is plotted as shown in Figure 10.

It may be noted at this time that each one of the curves appears to have a different slope. At first this might seem unreasonable since the slope of $|Z|$ versus $\log \omega$ should be constant for any parallel R-C circuit. The reason for the difference in slope can be easily seen by again considering $Z(j\omega)$ of the circuit:

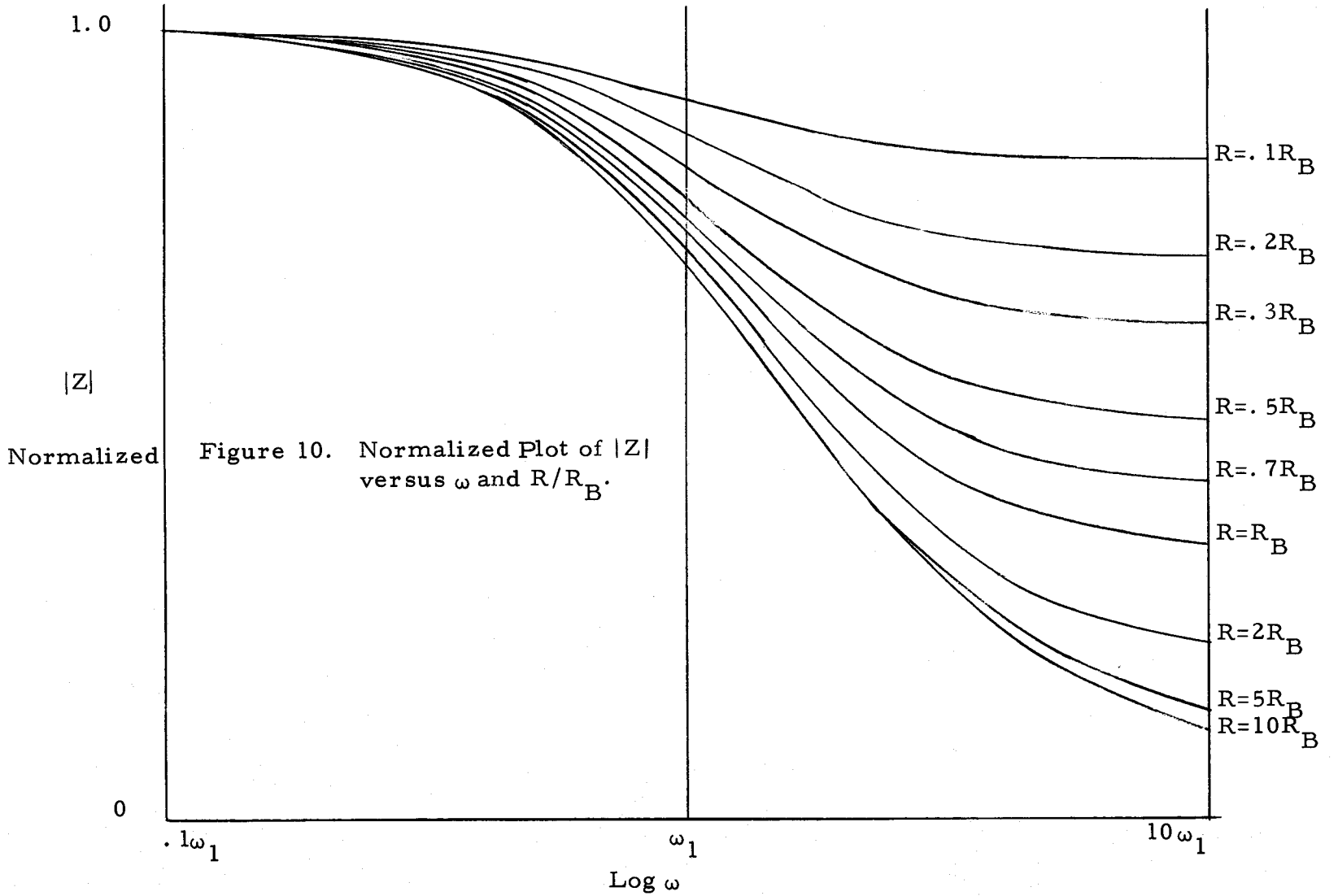

Figure 10. Normalized Plot of |Z| versus ω and R/R_B.

$$Z(j\omega) = \frac{jR_B RC\omega + (2R + R_B)}{jRC\omega + 1}$$

This function contains a break-point at $\omega_1 = 1/RC$ and a break-point at $\omega_2 = \frac{2R + R_B}{R_B RC}$.

An approximate plot of log $|Z|$ versus log ω can be made using the break-point method shown in Figure 11. The first break-point occurs at ω_1 and depends upon the RC time constant of the contact only. The asymptotic slope is shown and the dotted line indicates the shape of the impedance plot in the absence of ω_2. ω_2 is the second break-point at which the curve again becomes flat. The asymptotic curve as well as the shape of the impedance for the case of ω_1 far removed from ω_2 are shown. When these two break-points occur close together, they tend to change the impedance-versus-frequency plot as shown by the solid line. The closer together these points are, the smaller the slope of the plot. Thus, if ω_1 and the slope are known, the ratio of R/R_B is uniquely determined.

The main advantage of the family of curves is that if only a small portion of the curve is obtained, it can be compared to the given family of curves and a ratio of R/R_B determined. It isn't necessary, therefore, to include the frequency ω_2 in the data—though better accuracy is then possible. The only work involved in using these curves is in converting the data into a normalized curve for comparison purposes.

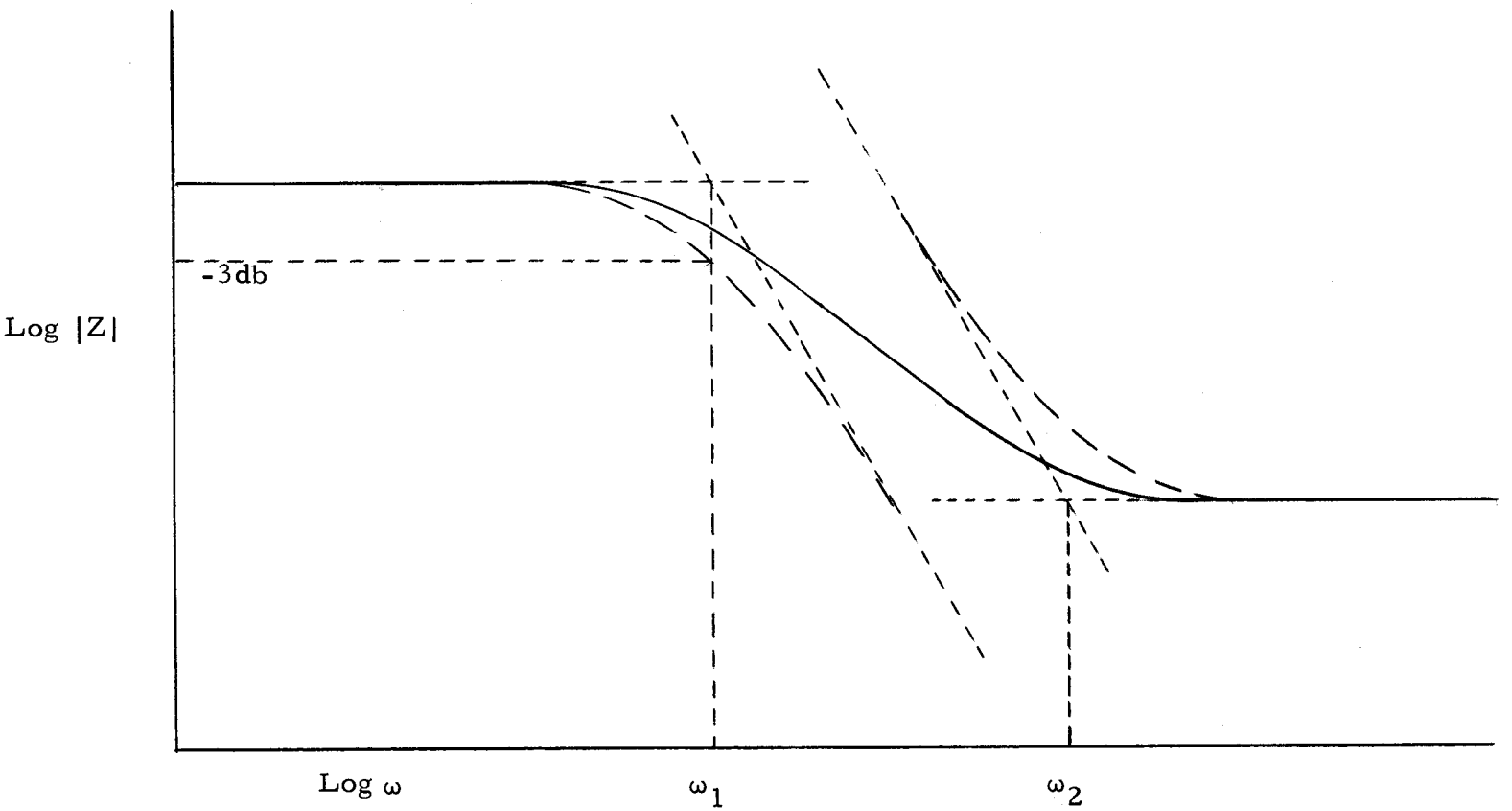

Figure 11. Break-Point Plot of |Z|

One other convenient measurement can also be made. Using the normalized curves, it is easy to establish a fairly accurate value of ω_1. C may now be calculated since $\omega_1 = 1/RC$. Without the curves, it would be difficult to determine the exact point at which ω_1 occurs since the -3 db point no longer falls at ω_1.

The magnitude of Z isn't the sole determining factor for finding the ratio of R/R_B. The phase angle of Z is plotted versus ω in Figure 12. It can be seen that the phase-angle curve has a unique maximum and general shape for each ratio of R/R_B. Thus, the ratio R/R_B may also be found by comparison of the phase-angle plots. It may be noted that the impedance curves tend to bunch together at values of R/R_B >5 and make determination difficult. However, the phase-angle curves show good separation for large ratios of R/R_B and allow accurate determination of the high ratios of R/R_B. For small ratios, the impedance curves are the most useful.

Both impedance and phase angle may be plotted together and compared simultaneously to the given curves. This method of comparison gives the best results and provides a cross check on the answer determined by each curve.

The basic method of measurement has been discussed for the ideal model. No frequency was specified since this will vary greatly depending upon the application and type of sample being measured. The actual application of this method to the measurement of contacts

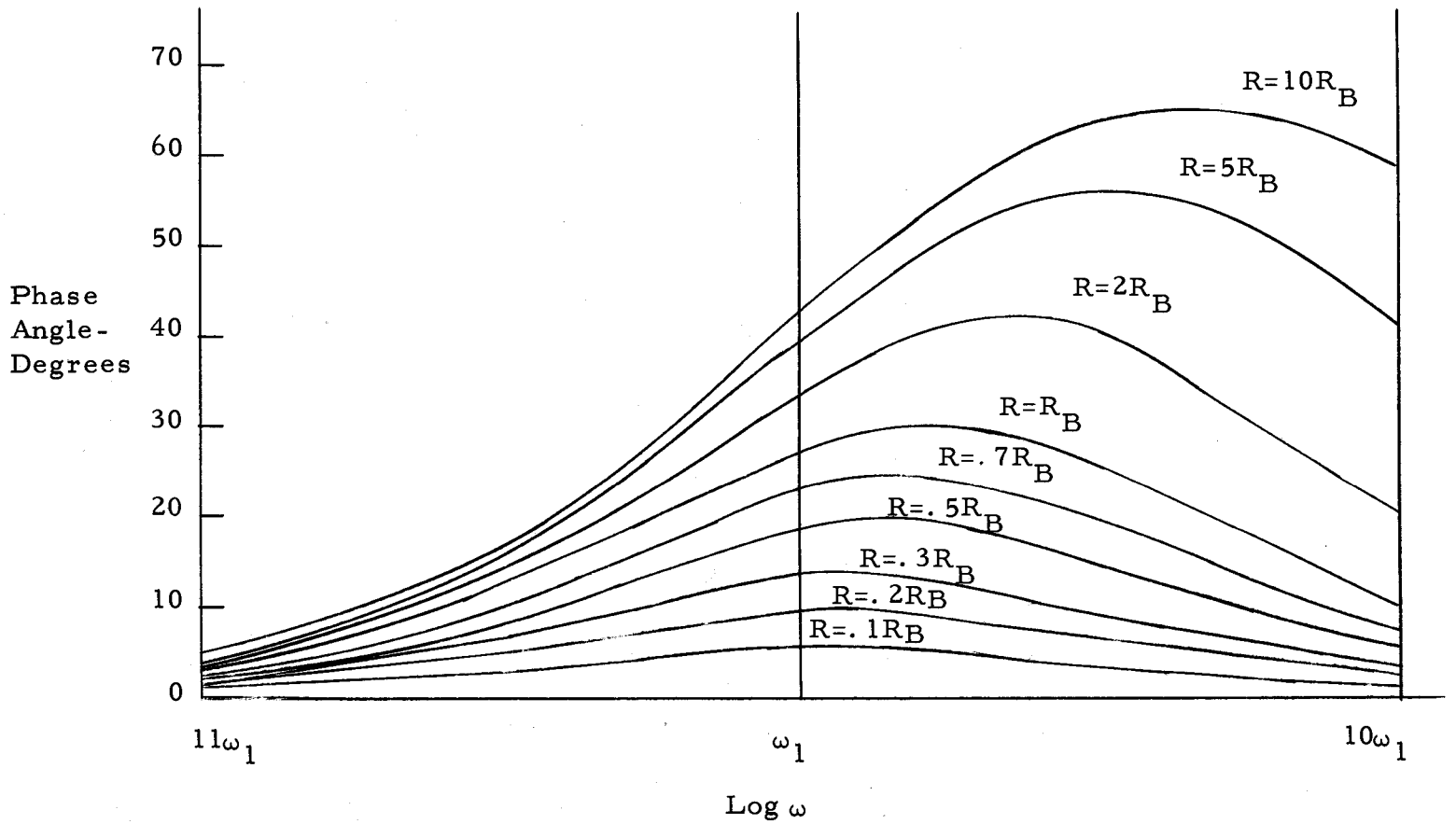

Figure 12. Phase Angle versus ω and R/R_B.

on a semiconductor needs some consideration since models are rarely perfect representations of the actual physical phenomena.

For the most part, the physical configuration supports the model. Any spreading resistance is included as part of R_B. Likewise, any other incidental circuit resistance will show up as part of R_B.

The shunting of the body resistance by the damage on the surface of the semiconductor due to sawing may be a problem with some semiconductors. However, this doesn't appear to be a problem with gallium arsenide since this surface layer is highly insulating[1] (8;9).

The easiest sample geometry to use is one which is similar to the model (See Figure 7). For this particular configuration, ω_1 doesn't depend on the area of the contact since $R \sim 1/A$ and $C \sim A$ such that the product RC is constant. However, ω_2 depends upon R_B. Any change in the dimensions changes R_B, the value of ω_2, and thus the shape of the impedance curve. This is quite reasonable since the shape of the curve depended upon R/R_B in the first place.

This places a limit on the sample dimensions. The thickness of the sample should be adjusted such that the expected ratio of R/R_B falls between 0.5 and 1. This results in a more accurate determination.

---

[1] Larry Bowman, Member of Technical Staff, Tektronix, Inc. Private Communication.

It is of interest to see how this method can be applied to the measurement of non-ohmic contacts.

There is a certain amount of capacitance and effective resistance due to the presence of the Schottky barrier. However, the values of capacitance and resistance aren't constant as was assumed by the model. Therefore, the impedance curves would be expected to have a different shape than those given previously.

This isn't a very large drawback since the value of R is arbitrary and varies as a function of voltage. The main determination which can be made is the value of R_B after the curve has become asymptotic at high frequencies. This value of R_B may then be used as a correction factor in the evaluation of the contact performance. Approximate average values may be estimated for R and C once R_B and the approximate ω_1 have been determined.

An interesting problem shows up in the barrier capacitance at VHF frequencies. At low frequencies, the capacitance of the barrier changes as a function of the applied voltage (11, p. 269). This is due to the widening of the depletion region with reverse bias and the corresponding narrowing under forward bias. As the frequency is increased, a relaxation phenomena takes place wherein the barrier width change tends to lag behind the applied voltage. The net result is a wider depletion region and an apparent reduction in the barrier capacitance.

This is an added deviation of the actual curve at high frequencies. However, this isn't serious since C wasn't considered constant.

The measurement of ohmic contacts is much easier since the ohmic contact closely approaches the assumed model. The contact resistance is considered analogous to a thin sheet of high-resistivity material placed between two conducting surfaces. Since the resistance of the contact doesn't vary with the applied voltage, it is apparent that the dimensions of the "sheet" remain unchanged. The capacitance of the contact then has the very simple relation given for two plane parallel plates. The "sheet" then acts as the dielectric between the plates. The capacitance of the contact is:

$$C = \frac{A\epsilon}{l}$$

where A is the area of the contact, ϵ is the dielectric constant, and l is the thickness of the sheet.

Since the thickness is constant, the capacitance will remain constant and won't change with the applied voltage or frequency as was the case with the non-ohmic contact.

An interesting effect of this model is that the RC time constant may be used to determine the bulk resistivity of the highly resistive "sheet" in the contact. The resistance and capacitance are related as shown below:

$$R = \frac{\rho_A l}{A} \qquad RC = \frac{(\rho_A l)}{(A)} \frac{(A\epsilon)}{(l)} = \rho_A \epsilon$$

$$C = \frac{A\epsilon}{l} \qquad \text{and} \qquad \frac{1}{\omega_1} = RC = \rho_A \epsilon$$

Since ϵ is a constant, ρ_A, the resistivity of the sheet in ohm-cm, is determined for any given measurement. If the value of ρ_A is relatively constant, then ω_1 will occur at about the same frequency for widely differing values of contact resistance.

The applicability of the model can be estimated by how well the experimental curve fits the theoretical curve. For the contacts reported in this paper, the fit was quite good indicating the validity of the assumptions which have been made.

One of the main advantages of the VHF bridge technique is that it only measures R. All other resistances are included in the term R_B. Also, the value of R_B doesn't need to be initially known and the measurement works well even on unhomogeneous material.

One of the major problems arises in trying to measure very small resistivities. VHF bridges require a correction procedure which isn't very accurate at low impedance levels. The resistance of the sample may be increased by adjusting its dimensions. However, if the sample resistance is still too low, then the potential-probe method should work satisfactorily due to the low resistivity of the material. Another limitation is the maximum frequency

capability of the bridge. In general, the bridge has to include at least ω_1 in order to determine R/R_B with any reasonable accuracy. In any determination, the minimum detectable results are determined by the accuracy of the bridge and the impedance correction procedure.

EXPERIMENTAL PROCEDURE

The preceding VHF bridge technique was developed in order to evaluate the contact resistance on high-resistivity gallium arsenide. Following this, several representative types of contacts were fabricated, measured, and compared.

Methods of Making Contact

A number of methods of making contacts were obtained from the literature and from personal correspondence with workers in the field. A complete list of these methods with their variations is contained in parts I and II of the appendix. It is interesting to note that each of the five individuals contacted used a different technique in making contact to P-type gallium arsenide even though they were all working in the injection-laser field which requires very low-resistance contacts. However, all of them used tin or a tin alloy in making contact to the N-type region. Tin acts as an N-type impurity and forms the heavily doped region required for an ohmic contact as described in the first section. Since the value of the tin contact on N-type material has apparently been established, this investigation was carried out on the several different methods of making contact to the P-type material.

In support of this approach, Minden stated that the main contact

problems lie in trying to make contact to the P-type region and indicated that a contact resistance of approximately one ohm exists in the P contact to the heavily doped injection lasers (23, p. 40). Another reason for the choice of P-type material was the consideration of sample resistance. The available N-type material had a resistivity of about 0. 1 ohm-centimeters while the P-type material had a resistivity of about 2 ohm-centimeters. This increased resistance results in better bridge accuracy as pointed out earlier.

The basic methods of making contacts to the P-type gallium arsenide fall into two general categories - plated contacts and alloyed contacts.

One type of plated contact is nickel[1] which is either vacuum deposited or applied by electroless-plating techniques. The nickel plating is then often covered by a gold evaporation to prevent oxidation of the nickel. A heat treatment is usually included since this is found to lower the resistivity of the contact (19;32).

Another type of plated contact is silver[2] which may be vacuum evaporated or electroplated onto the sample. Again, a gold evaporation may be used to protect the silver during soldering. As in the

---

[1] Arnold, K., Member of Staff General Telephone and Electronics Laboratories. Private Communication.

[2] Quist, Theodore M., Member of Staff Lincoln Laboratories. Private Communication.

case of the nickel, a heat treatment is often used to improve the contact resistance (6).

In some of the alloyed contacts, zinc is used either as the main contacting agent or as the P-type impurity in a metal alloy contact. Zinc alloys which are often used include indium-zinc alloys,[3] lead-silver-zinc alloys, silver-zinc alloys,[4] and gold-zinc alloys. In using zinc, the ohmic contact is apparently formed as a result of the heavily doped P region formed at the surface of the gallium arsenide with zinc as the impurity. Alloying usually takes place using a vacuum-evaporated layer of the alloy metal (4;7;13;23).

Aluminum and indium are two other contact materials which are used (32;5;21;18). The alloyed contact is usually from a plated source.

The above contacting methods are the ones most often used. Gold, which is used in work with silicon and germanium, is sometimes used in making contact to gallium arsenide. However, it is suspected that this is a carry over from germanium and silicon device technology. Previous investigations with gold contacts indicate very high resistances.

---

[3]Hall, R. N., Member of Technical Staff, General Electric Research Laboratory. Private Communication.

[4]Archer, R. J., Member of Staff, Hewlett Packard Associates. Private Communication.

The plated contacts listed above require a lapped surface for the formation of an ohmic contact in accordance with the theory presented by Hunter. As explained earlier, the alloyed contacts form ohmic contacts by heavily doping the semiconductor near the surface.

In conducting a comparison of contact types, the contact which was felt to be representative of that type of contact was selected from each of the five groups listed above. It must be recognized at this time that minor variations in the technique of applying these contacts may result in a considerable variation in the answers obtained. Each of the five general methods may be considered as a grouping of a considerable number of individual methods of making contact. The methods listed in the appendix will give an idea of the possible variations in technique.

To help provide a better comparison, each type of contact received essentially the same surface preparation prior to the application of the contact. The contact preparation used for each of the samples is given below.

The original material was P-type with the following specifications:

$$\rho = 1.8 \text{ ohm-cm}$$

$$\mu = 230$$

$$N_a = 1.5 \times 10^{16} \text{ acceptors/cm}^3$$

All contacts were applied to the $\bar{1}\bar{1}\bar{1}$ faces and the 111 faces of a prepared wafer which was about 0.5 cm wide x 1 cm long x 0.04 cm thick. Each wafer yielded from five to twenty finished samples. The wafers were first lapped with #600 SiC in order to remove all saw damage and to provide an essentially flat surface. Then the wafers were rinsed and lapped with 1 micron alumina to remove the surface damage caused by the larger #600 grit. The wafers were rinsed again and polished using 0.05 micron alumina. Immediately following this, the wafers were thoroughly washed in deionized water using the ultrasonic cleaner for a duration of about five minutes. Following the cleaning process, one of the two wafers being processed was etched in a solution of three parts H_2SO_4, one part H_2O_2, and one part H_2O in order to remove the lapping damage. The two wafers were carried along together to check on the effect of a lapped surface versus an etched surface.

In all of the above lapping procedures, rubber gloves were used to help prevent contamination. All rinsing was done using deionized water. After etching, the two wafers were kept in methyl alcohol until the contacts were applied. More extensive cleaning of the wafers was not attempted in order to prevent the possibility of further exposure to the atmosphere and additional sources of contamination. It is assumed that the freshly lapped surface was adequately clean. The main impurity present was the lapping compound which should

be pretty well removed by the ultrasonic cleaning process. The inclusion of any of the alumina shouldn't be harmful due to the refractory nature of the material which is relatively inert at the temperatures being used.

After completing the surface preparation procedure listed above, the five separate contacts were applied as follows.

One of the plated contacts investigated was the electroless-nickel plated contact with a heat treatment. In order to successfully plate nickel on gallium arsenide, a predip procedure must be used in order to catalyze the nickel reduction in the nickel-plating process (26). In this procedure, the wafer is dipped in a $SnCl_2$ solution @90°C for one minute. Following this, the wafer is rinsed and dipped in a $PdCl_2$ solution @90°C for one minute. The wafer is then rinsed and is ready for plating.

The nickel plating is carried out in the standard electroless-nickel plating bath often used for applying contacts to silicon (26). The plating time is about two minutes at 95°C. During this time, the solution is kept slightly basic by the addition of ammonium hydroxide.

Following the plating process, the wafer is heat treated in an atmosphere of forming gas (90% N_2, 10% H_2). The strip heater is used and the wafer is held at approximately 400°C for about 15 minutes. Following the heat treatment, the wafer is once again nickel plated and is ready for cutting up into the appropriate size samples

for measuring.

The other plated contact was a silver contact. Two separate runs were made with minor variations in the procedure. The resulting contacts were essentially identical, however, and were measured together.

The first set of wafers was vacuum deposited with about 0.5 microns of silver and about 0.5 microns of gold over the silver. This was done on each side in turn. The approximate depth of the plating was calculated by assuming the plating metal as a point source and the sample as part of the inside surface of a sphere with a radius of about two centimeters. The film thickness may then be approximated if the volume of the total evaporated metal is known.

Following the silver and gold plating, the wafers were heat treated in an atmosphere of forming gas at 200^{o}C for about fifteen minutes. They were then ready for dicing.

The second run received the same silver and gold plating. However, the wafers weren't heat treated but were nickel plated instead. Several of the diced samples were later given the same heat treatment described above. Strangely enough, the heat treatment tended to increase the resistance slightly.

A contact was selected from the zinc-alloy group which was representative of what might be expected using zinc as an impurity. The sample preparation followed the procedure given previously. The

etched and the lapped wafers were then plated with a gold-zinc alloy on both sides to a total depth of about one micron. Zinc plating alone presented a few problems. Zinc itself won't wet a tungsten filament and is very difficult to contain in the molten state. When the zinc was evaporated, it tended to plate preferentially. The effect was a spot of zinc here and there which was unusable. It was found that a higher application rate tended to help somewhat, but then the zinc would jump out of the filament.

To help overcome these problems, the zinc and the gold were plated together. When heated up, they tended to form an alloy. Then the zinc was vaporized first due to its much lower vapor pressure. The result was a layer of zinc on the gallium arsenide. Then the filament temperature was raised further and the gold was evaporated over the zinc. The procedure seemed quite satisfactory.

Following the plating process, the wafers were alloyed on the strip heater in an atmosphere of forming gas. The alloying was done at a temperature between 500° and 600°C. Following the alloying, the wafers were nickel plated to ensure good ohmic contact to the gold-zinc alloy. The wafers were then ready for dicing.

An aluminum contact was also made. The same surface preparation was carried out. About one micron of aluminum was vacuum evaporated on each side of the wafer following which the wafer was nickel plated lightly prior to alloying. The purpose of

this initial nickel plating is to help the aluminum wet the surface of the gallium arsenide so that a good, uniform alloying takes place. Without the nickel plate to hold the aluminum in intimate contact, it was felt that the aluminum might tend to melt and form small spheres on the surface of the gallium arsenide without alloying properly.

The alloying was done on the strip heater in a forming gas atmosphere. The alloying process was checked visually and was considered complete when a noticeable uniform change occurred in the appearance of the surface. The wafer was again nickel plated to help improve the contact and was then ready for dicing.

The final contact which was investigated was an indium contact. The same surface preparation was carried out and etched and lapped wafers were carried through the process. About one micron of indium was vacuum evaporated on each side. The wafers were then nickel plated for the same reason given previously for the plating of the aluminum. The wafers were alloyed at about 350°C on the strip heater in an atmosphere of forming gas. Following this, the wafers were ready for dicing.

VHF Bridge Adaptation

Once the contacts were made, they were evaluated using the VHF bridge method described in the preceding section. One consideration was the selection of the sample size. The thickness of the

wafers was about 0.35 mm. The resistivity was about 2 ohm-centimeters. A sample one mm square would then have a resistance of about 6 ohms. Allowing for a total contact resistance of about equal value, the total resistance would be about 16 ohms which was about the right magnitude for relatively accurate use of the bridge. The most convenient method of preparing the one mm samples was to saw up the wafers prepared earlier using a diamond saw (320 grit - 100 concentration). This gave a number of uniform samples which allowed more than one measurement on a contact type as a check on the contact uniformity and the measurement accuracy.

The bridge which was used for the impedance measurements was the Hewlett-Packard model 803-A VHF bridge. The important specifications of this bridge are listed below:

Useful frequency range	5 - 700 mc
Impedance range	2 - 2000 ohms
Phase angle above 50 mc	-90° to $+90^{\circ}$
Phase angle accuracy	$\pm$ 3 degrees
Impedance magnitude accuracy	5%

In conjunction with this bridge, the following auxiliary equipment was used:

Signal generator	Hewlett Packard Model 608A
VHF Detector	Hewlett Packard Model 417A

These units have a frequency range of 10 to 500 mc.

The "unknown" terminal of the bridge is a female type-N connector. A suitable sample holder was designed which would hold the one mm square sample, would allow easy changing of samples, and which was usable at frequencies up to 500 mc. At VHF frequencies, stray capacitance, lead inductance, or impedance mismatches with the 50 ohm input impedance of the bridge present problems in obtaining accurate, reproducible measurements. A cut-away view of the holder is shown in Figure 13.

The sample holder was built into a type N male connector. A copper spring was soldered to the center wire as shown. The sample was then held between the copper spring and a flat copper plate soldered to the inside of the connector.

Following are some of the desirable characteristics of the sample holder. The connector is of minimum length so that a minimum amount of error will be introduced due to line losses. The connector itself should approximate a continuation of the 50 ohm line within the bridge. The end of this line is terminated in the sample to be measured which is the way the bridge was designed to operate. The sample holder itself is of rigid and compact construction and the sample is held securely in a predetermined position thus contributing to the accuracy and reproducibility of the results. The copper spring and copper plate should ensure reasonably good low-resistance contacts to the sample. As may be seen, stray capacitance is held to a

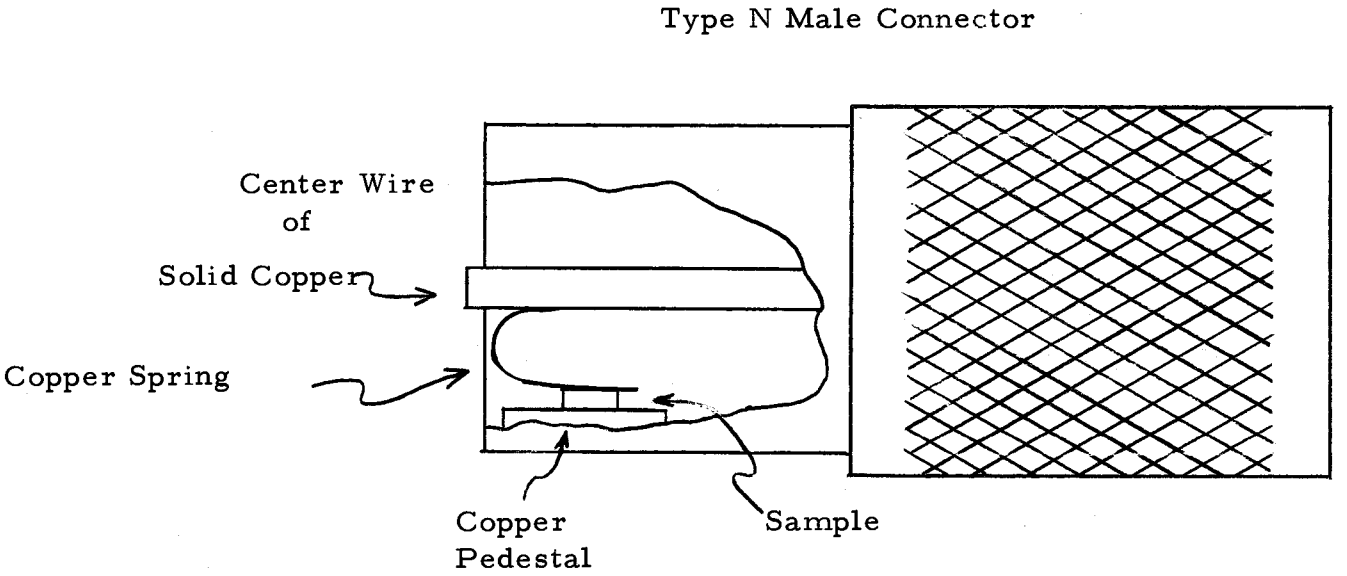

Figure 13. VHF Bridge Sample Holder.

minimum and is essentially determined just by the area between the spring and the plate. The calculated value of C stray is about 0. 5 pf with the sample in place. This is about 700 ohms at 500 mc and is still negligible compared to the sample resistance of about 10 ohms. The rest of the "stray" capacitance is part of the characteristic impedance of the transmission line.

The operating instructions for the bridge indicated that an equivalent circuit could be used as a correction factor for unknowns connected directly to the terminals. However, the use of this circuit resulted in a considerable error.

Instead, an electrical wave length λ versus frequency plot had to be made such that the Z - θ chart supplied with the bridge could be used. The Z - θ chart is similar to the Smith chart in that it allows the determination of an impedance at the end of a length of transmission line providing that the impedance and the electrical length of the line are known at the point of measurement.

To obtain the λ correction versus frequency for the sample holder and the bridge, it was necessary to place a short at the point of measurement. Knowing that the termination was zero impedance, a correction λ could be calculated. The short was made using a piece of copper with the same dimensions as the samples being measured. Thus, the dimensions of the holder wouldn't change and the correction curve could be assumed to be accurate.

In the bridge specifications, an angle accuracy of $\pm$ 3 degrees was given. This resulted in an error greater than 10% in the magnitude of the impedance above about 150 mc and showed up as a periodic variation of the data points. To help eliminate this error, the known phase angle of 90° was measured using the copper shorting blank. Then any variations noted in the actual measurements were plotted as a correction angle at 90°. Impedance angles less than 90° may be interpolated by assuming no error at zero degrees.

In calculating the actual impedance from a measured value, the angle correction was first made. Then the Z - θ chart was used to find the value of the sample impedance. This impedance was normalized to the low-frequency value so that it could be plotted and compared to the theoretical set of curves. The phase angle was also plotted on the same graph and gave an additional check on the R/R_B ratio being determined.

Measurement Procedure

A fixed procedure was used in measuring each type of contact. Each individual sample for each contact type was checked for linearity. The resistance of the sample was read directly if the V-I characteristic was linear. If it wasn't linear, then a reference measurement at $\pm$ 0.5 volts was chosen and the average resistance over this voltage range was listed as the sample resistance.

The linear samples were then measured on the bridge as a function of frequency. A few check-points were plotted for each contact type to determine the break-point frequency. Then the majority of the data was taken so as to most accurately determine the shape of the curve. In all cases of ohmic contacts, the value of the resistance measured on the Tektronix type 575 curve tracer was within 5% of the value measured on the bridge.

The non-linear samples were assumed to contain a barrier region and were measured with the assumption that the ohmic-contact model didn't apply. The only measurement made on these samples was to determine the value of R_B. The results were consistent and good asymptotic curves were obtained at high frequencies.

The evaluation of the experimental data will be given in the following section.

EVALUATION OF MEASUREMENTS

Statistical Evaluation

The measurement of each set of samples was carried out essentially as given in the last section. Each set was completely checked for the range of total resistance. Then a representative sampling of the different total resistances was chosen for the impedance versus frequency measurement. This method of sampling was done in order to see if the variation in total resistance was due to a variation in the contact resistance or to a variation in the body resistance.

The data which was taken for the linear contacts was plotted on three cycle semi-log paper and compared to the theoretical curves in order to determine the values of R/R_B, ω_1 and R_{total}. From these values, R, R_B, and C were calculated. The total results are tabulated in part III of the appendix. The values of R and R_B were found by solving the two simultaneous equations:

$$R_{total} = 2R + R_B \text{ and } R/R_B = K$$

where K is the determined value of the ratio R/R_B. The contact capacitance was calculated from the definition of $\omega_1 = 1/RC$.

In the case of the non-linear contacts, the data was taken in order to determine R_B. R, C, and ω_1 are all variable and weren't calculated as such. The only other measurement made was R_{total} as

explained in the previous section. R_{total} and R_B are tabulated in parts IV and V of the appendix.

The data which was taken needed to be reduced to a usable form for comparison purposes. Geometry shouldn't be a factor in any comparison of two values. Thus, the contact resistivity, ρ_c, may be calculated if the resistance and the contact area are known. It has the units of ohm-cm^2 and allows the easy computation of any contact resistance of known area.

The average resistivity for each contact type is relatively easy to compute and allows a rough comparison between contact types. For a better comparison, some information is needed concerning the variation of the resistivity of each type of contact. One way of representing this is to specify a percent error for each resistivity. However, this doesn't indicate the variation which might be expected for the rest of the samples.

The variance or the standard deviation gives a better measure of the variation, but may be a little difficult to interpret quantitatively. A better method of presenting the results is to establish a confidence interval of the contact resistivity. A 95% confidence interval may be considered as the resistivity range which has a 95% probability of including the true mean of the contact resistivity for any of the contact types being measured. The use of the confidence interval is found in comparing two different contacts. If two different confidence intervals

don't overlap, then it is apparent that the mean resistivity of the two contact types is different. Any overlapping of the confidence intervals suggests the possibility of identical means and can't be considered conclusive evidence for stating that a difference does exist.

A confidence interval is set up using standard statistical-inference techniques. In this case, the t statistic was chosen since the sample variance was estimated from the sample itself. The assumption was made that the samples measured came from a normal population.

A confidence interval was calculated for the mean contact resistivity of each of the linear samples and for the body resistance measured for the non-linear samples. Also, in the case of the non-linear samples, a comparative value of the average contact resistivity at ± 0.5 volts was calculated and a confidence interval established. The average values of each of these contact resistivities and their associated confidence intervals are contained in Tables I and II. Figures 14 and 15 show the graphical representation of the confidence intervals of the contact resistivities of the linear and non-linear contacts.

The data also indicated another interesting relationship. Figure 16 shows the plot of 1/R versus C. The shape of this plot indicates that C and R are inversely related by the equation $C = B/R + D$ where B is the relationship between C and 1/R and D is a constant. In the previous section (page 39) the mathematical and physical meaning

TABLE I. CONTACT RESISTIVITIES FOR THE LINEAR CONTACTS

Contact type	$\bar{\rho}_c$-ohm cm^2	95% Confidence interval of ρ_c-ohm cm^2
Al - lapped	3.54×10^{-2}	$2.91 \times 10^{-2} < \rho_c < 4.16 \times 10^{-2}$
Zn - lapped	1.8×10^{-2}	$1.62 \times 10^{-2} < \rho_c < 1.98 \times 10^{-2}$
Zn - etched	0.345×10^{-2}	$0.059 \times 10^{-2} < \rho_c < 0.631 \times 10^{-2}$

TABLE II. AVERAGE VALUES OF CONTACT RESISTIVITY AT $\pm .5$ VOLTS FOR NON-LINEAR CONTACTS

Contact type	R_{total}-ohms	$\bar{\rho}_c$-ohm-cm^2	95% Confidence Interval of ρ_c-ohm-cm^2
Ag - lapped	36	.248	$.178 < \rho_c < .319$
Ag - etched	365	3.28	$0 < \rho_c < 11.4$
Ag - lapped*	29	.184	$.0962 < \rho_c < .272$
Ag - etched*	1833	16.8	$6.56 < \rho_c < 26.9$
Ni - lapped	34	.230	$.208 < \rho_c < .252$
Ni - etched	269	2.39	$.875 < \rho_c < 3.91$
Indium	7.6K	70	$25.8 < \rho_c < 114$
Heat treated*			
Body Resistance			
R_B-ohms		9.02 ohms	$8.6 < R_B < 9.4$ ohms

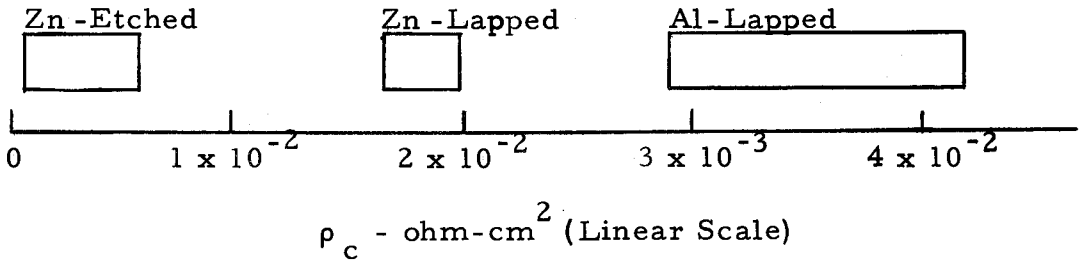

Figure 14. 95% Confidence Intervals of The Linear Contacts.

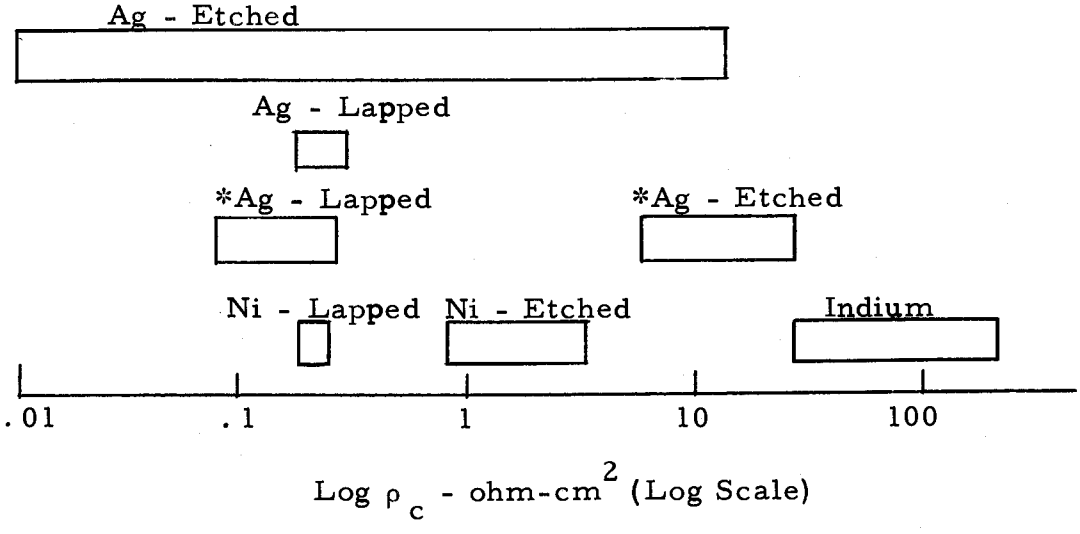

*Heat treated

Figure 15. 95% Confidence Intervals of the Non-Linear Contacts.

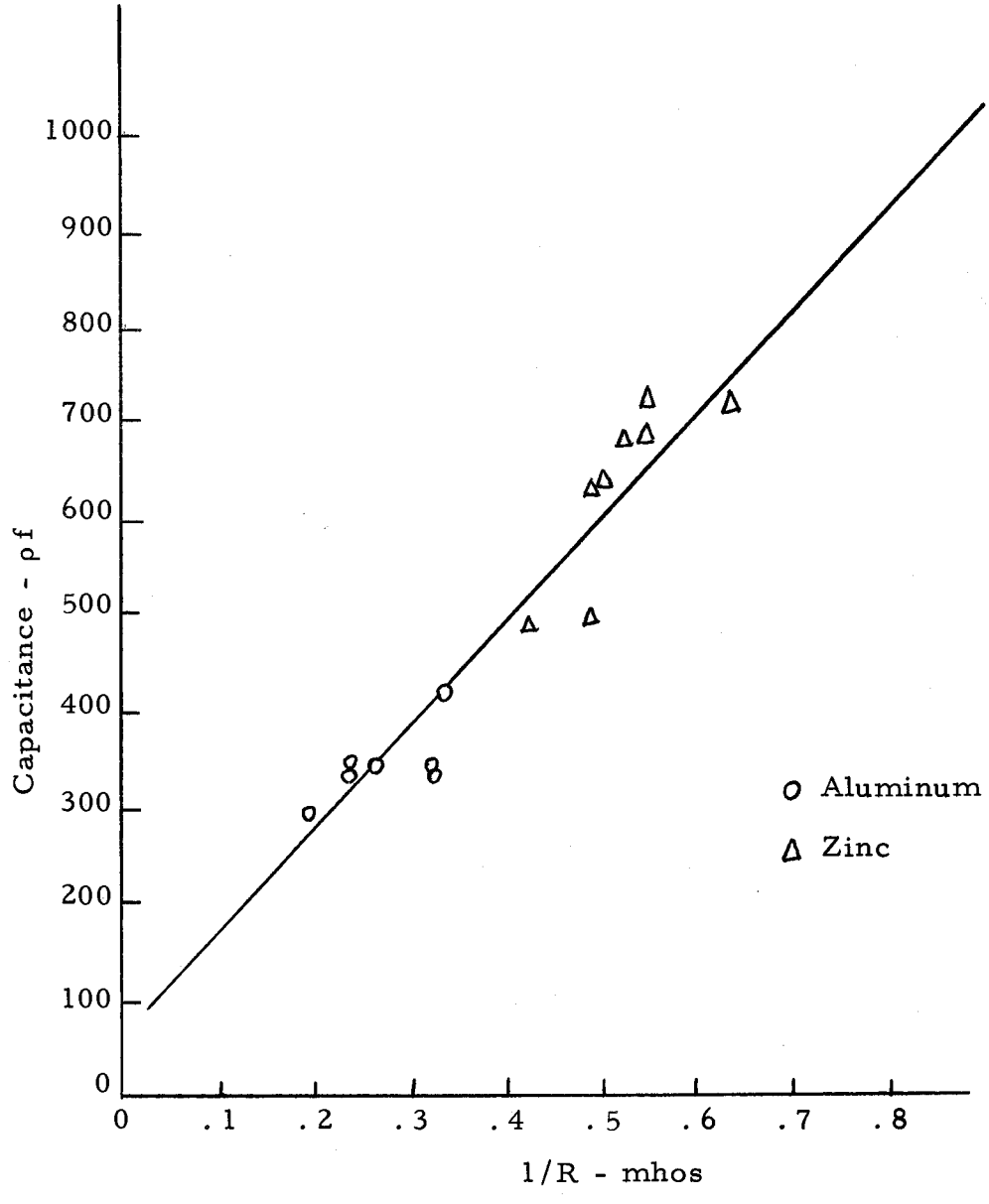

Figure 16. Contact Capacitance Versus 1/Contact Resistance.

of the dependence of C and 1/R was shown. The results indicated that $\rho_A \epsilon = B$ where ρ_A is the resistivity of the highly resistive region in the contact.

To test for this relationship, linearity was assumed over the range for which the data is available. Again using statistical techniques, a test was run which is designed to test the hypothesis that the slope of the line, B, is equal to zero. A rejection of this hypothesis would indicate that B had a positive value and would certainly indicate a relationship between C and R.

The results of the test indicated that the value of B was contained in the following 95% confidence interval:

$$864 < B < 1320$$

The mean value of B calculated from the data using the method of least squares was B = 1092. The confidence interval indicates a definite correlation between the contact capacitance and the contact resistance since the value of B = 0 was not contained within the established confidence interval.

The capacitance and resistance may also be related by the following expression:

$$C = \frac{1092}{R} + 64 \text{ pf}$$

It is now possible to calculate ρ_A knowing B.

$$\rho_A = \frac{B}{\epsilon} = 1100 \text{ ohm-cm}$$

This is the approximate resistivity of the resistive sheet given by the model presented for the contact resistance. The thickness of the resistive sheet may be found for any given resistivity by the following expression:

$$\text{Thickness} = \frac{\rho_c}{\rho_A} \text{ cm}$$

For a sample with a 1 ohm contact resistance, ρ_c would be 10^{-2} ohm-cm^2 and the thickness of the resistive region would be:

$$T = \frac{10^{-2} \Omega\text{-cm}^2}{1.1 \times 10^3 \Omega\text{-cm}} = .9 \times 10^{-5} \text{cm} = 900 \text{ Angstroms}$$

This thin region explains the high capacitance which was measured.

Error Analysis

An evaluation should be made of the overall worth of this measuring procedure in light of the results presented thus far. The statistical techniques themselves are reasonably sound. Of course, there

are always exceptions as allowed for by the 95% confidence placed upon the answers. The possible errors in the measurement include: variations in sample geometry, accuracy of the bridge and accuracy in reading the bridge, correcting the data by use of the Z - θ chart, plotting the data, and determining the ratio of R/R_B from the plot. The value of R_B may be taken as somewhat of an indication of the accuracy which might be expected from this measuring technique. The range of R_B is about 0.8 for an average of 9 ohms. This represents about 10% error. The sample sizes were fairly constant for these particular samples indicating that the inaccuracy may be primarily attributed to the measurement technique. In the case of measuring only R_B as above, some error is eliminated by not having to estimate a value of R/R_B from the given curves. This should be expected to introduce a somewhat larger error in the results for the contact resistance.

The confidence intervals for the linear contacts were wider indicating a larger possible margin of error. However, the width of the confidence interval depends on the number of observations involved and as such can't be accurately used as an estimation of error. The accuracy of determining the contact resistivity should involve no more than 15% error. An apparent error in excess of this is most likely due to an actual difference in the contacts themselves. It is quite probable that a difference of at least 15% may be found between

the contact resistivities of identical contacts determined by two separate runs. This would be primarily due to the minor differences in technique which occur. Of course, this source of error can be reduced to a certain extent by very careful technique.

One experiment was done on four of the five methods of making contact and two experiments on the fifth method. A confidence interval of the contact resistance was set up for each of these contact types. The confidence interval thus established applies only to that particular experiment, and not necessarily to the method of making contact. In order to make any statistically sound predictions about any one contact type, a number of different trials should be made such that the variance of the different trials, including minor differences in technique, might be estimated.

The conclusions which have been reached for the different types of contacts do have some basis, however. Preliminary investigation on different experimental runs of aluminum, nickel, and zinc contacts indicated results similar to those reported in this paper. The silver contact was duplicated twice and is included in the data. On the basis of the previous investigations, the comparisons appear to be representative.

Theoretical Justification of Results

A theoretical justification of the results obtained can also be

made. The two methods of making plated contacts showed non-linear V-I characteristics indicating the existence of a barrier. This might be explained by the role of the surface states in forming a barrier in a plated contact.

An appreciable difference was noted between the lapped and etched surfaces. In all cases of the plated contacts, the lapped surface resulted in a much lower resistance than the etched surface. The etched surface also showed quite a bit of non-linearity while the lapped surface resulted in an almost linear V-I characteristic. This is to be expected since a lapped surface is often used in the formation of an ohmic contact (14, pt. 3, p. 15).

The zinc contact and the aluminum contact both showed the expected behavior. Apparently no barrier existed and the resistive-sheet model was applicable. The contacts were linear with a low resistance indicating that alloying took place for both the etched and the lapped samples.

The etched-zinc contact showed an appreciably lower resistance. One explanation is a cleaner contact which should result in better and more complete alloying without included impurities. The capacitance and resistance indicated the formation of a much narrower resistive region. This may be also explained by the fact that lapping damage was removed probably resulting in a thinner contact region. In the case of the lapped surface, the thickness of this resistive region

may be partially determined by the depth of the lapping damage.

The indium contact indicated the existence of a barrier shunted by a wide resistive region. This behavior of indium might be expected since it comes from the same column in the periodic chart as gallium and doesn't act like a P-type impurity in gallium arsenide even though it will change the band structure near the surface. Adequate evidence of the formation of an alloy is given by the fact that both the lapped and etched samples were identical after being alloyed.

An interesting variation of R_B with the zinc and the aluminum contacts was found. In the case of the zinc contact, R_B varied considerably but tended to be less than the value of nine ohms determined for the plated contacts. The reduced value is reasonable when considering the light doping level of the gallium arsenide. Zinc has a very high diffusion rate in gallium arsenide. During the alloying process, it is quite probable that an amount of zinc sufficient to change the body resistance diffused into the semiconductor. Apparently this diffusion wasn't homogeneous as seen by the variation in R_B. However, variations in R_B weren't important since the contact resistance was the value being measured. The confidence interval indicates only a small variation in the measured contact resistance.

In the case of the aluminum, the body resistance was higher. This could be the result of several factors. One is the inclusion of some impurity in the alloy source which would tend to raise the

resistance of the bulk semiconductor. A more likely explanation is the existence of a series resistance due to either a poor contact or a plating which is too thin on the surface of the sample. If the plated metal has a high resistivity or is too thin, the resistance from the copper spring to the actual contact resistance will be increased and will appear as part of the bulk resistance. This distributed resistance isn't frequency dependent in the range considered and can thus be ignored in determining the contact resistance. As in the case of the zinc, the aluminum contact resistance appeared to be constant indicating the validity of the measurements.

The relationship for capacitance versus resistance gave support to the model of a highly resistive region. In this model, the thickness of the slab goes to infinity as resistance goes to infinity. This should cause the capacitance to go to zero which would correspond to $C = 0$ for $1/R = 0$. The graphically determined C at $1/R = 0$ was about 65 pf. This isn't large compared to the capacitances involved. It might be noted that the requirement that $C = 0$ when $1/R = 0$ is within the confidence interval of B. Another consideration is the fact that C versus $1/R$ was computed for only a certain range of values. It is entirely possible that B isn't constant which would be the case where ρ_A doesn't remain constant.

Another departure of the dependence of $1/R$ and C would occur with very narrow regions where the recombination region would no

longer be wide compared to the diffusion length of the carriers, and thus the model would lose its effectiveness. However, conclusions beyond this point would require further investigation outside of the scope of this paper.

CONCLUSIONS

The theory of metal-semiconductor contacts was applied to contacts on gallium arsenide. The existence of a finite ohmic-contact resistance was explained by Hunter (14, pt. 3, p. 14) in his model which proposed a sandwich made up of the metal contact, a highly resistive region with a very high recombination rate, and the bulk semiconductor.

Any evaluation of this contact resistance requires an accurate means of measurement. Several more common methods were proposed but weren't found to be applicable to high-resistivity gallium arsenide. To overcome this, a method using a VHF bridge was developed. The model presented for the contact is a parallel R-C circuit which acts as a short circuit at high frequencies. A comparison of the low and high frequency values of impedance allows a determination of the contact resistance. To facilitate measurements, a set of theoretical curves was plotted and used.

The samples investigated were chosen to be representative of some of the different methods of applying the contacts. These contacts were then evaluated and were analyzed using standard statistical techniques. A comparison of the methods of making contact shows the following conclusions:

1. Alloyed contacts, with the exception of indium, have lower contact resistivity with the zinc-etched contact

being the best.

2. The plated samples resulted in reasonably low resistance contacts even though they weren't linear. Silver proved to be somewhat superior to nickel. Lapping is necessary in making a low-resistance plated contact.

3. Evidence was found to support the model that an ohmic contact is a narrow, highly resistive region which is shunted by an equivalent capacitance. A definite relationship was found between the contact capacitance and the contact resistance.

BIBLIOGRAPHY

1. Allen, J. W. The reverse characteristics of gallium arsenide P-N junctions. Journal of Electronics and Control 7:254-260. 1959.

2. Bardeen, J. Surface states and rectification at a metal semiconductor contact. Physical Review 71:717. 1949.

3. Blanc, J. and L. R. Weisberg. Energy-level model for high-resistivity gallium arsenide. Nature 192:154-165. October 14, 1961.

4. Broom, R. F. Room temperature operation of gallium arsenide lasers. Physics Letters 4:330-331. May 15, 1963.

5. Casey, H. C., Jr. Fabrication of gallium arsenide subnanosecond switching diodes. Stanford, Stanford University, Dept. of Electrical Engineering, May 1962. 27 p. (Stanford Electronics Laboratories Technical Report no. 1802-1).

6. Cunnell, F. A. et al. Technology of gallium arsenide. Solid State Electronics 1:97-106. 1960.

7. Dale, J. R. Simple ohmic contacts on gallium arsenide. Solid State Electronics 6:388-390. 1963.

8. Gatos, H. C., E. P. Narkois and M. C. Lavine. Surface damage in III-V compounds ($\overline{111}$) surfaces. Journal of the Electrochemical Society 107:199C. August 1960.

9. Gatos, H. C., E. P. Narkois and M. C. Lavine. Characteristics of the ($\overline{111}$) surface of the 3-5 intermetallic compounds. Part 2. Journal of the Electrochemical Society 108:645-649. July 1961.

10. Hannay, N. B. Semiconductors. New York, Reinhold, 1959. 767 p.

11. Henisch, H. K. Rectifying semi-conductor contacts. London, Oxford University Press, 1957. 373 p.

12. Hill, Dale. Evaluation of the Hall coefficient and resistivity of gallium arsenide. Semiconductor Products 5:29. 1962.

13. Holoynak, N. and J. A. Lesk. Gallium arsenide tunnel diodes. Proceedings of the Institute of Radio Engineers 48:1405-1409. 1960.

14. Hunter, Lloyd P. Handbook of semiconductor electronics. York, Pa., McGraw-Hill, 1956. 20 sections.

15. Larrabee, Graydon. The contamination of semiconductor surfaces. Journal of Electrochemical Society 108:1130-1134. 1961.

16. Lark-Horovitz, K. and Vivian A. Johnson. Methods of experimental physics. New York, Academic Press, 1959. 416 p.

17. Lavine, Jerome M. GaAs injection lasers. IBM Journal 7:17-20. January-February 1963.

18. Loebner, E. E. Hewlett Packard Associates interim engineering report no. 3, March 1, 1963 to May 1963. Palo Alto, California. 63 p. (Air Force Contract No. Af33(657)-9772, BPSN: 3-6799 760E 415906).

19. Logan, R. A. et al. Avalanche breakdown in gallium arsenide P-N junctions. Physical Review 128:2518-2523. 1962.

20. Lowen, J. and R. H. Rediker. Gallium arsenide diffused diodes. Journal of the Electrochemical Society 107:26-29. 1960.

21. Lucovsky, G. and P. H. Cholet. Gallium arsenide, a sensitive photodiode for the visible. Journal of the Optical Society of America 50:979-983. 1960.

22. Mead, C. A. Metal contact double injection in GaAs. Proceedings of the Institute of Electrical and Electronics Engineers 51:954-955. 1963.

23. Minden, Henry T. Gallium arsenide electroluminescent and laser diodes. Semiconductor Products 6:34-48. August 1963.

24. Nathan, M. I. et al. Stimulated emission of radiation from GaAs P-N junctions. Applied Physics Letters 1:62-64. November 1, 1962.

25. Nibler, F. Some properties of ohmic metal-semiconductor contacts. Journal of Applied Physics 34:1572. 1963.

26. Pearlstein, Fred. Electroless nickel deposition. Metal Finishing 1:59-61. August 1955.

27. Sharpless, W. M. High frequency gallium arsenide point-contact rectifiers. The Bell System Technical Journal 38:259-269. 1959.

28. Shive, John N. The properties, physics, and design of semiconductor devices. Princeton, D. Van Nostrand, 1959. 487 p.

29. Smith, R. A. Semiconductors. Cambridge, University Press, 1961. 496 p.

30. Spitzer, W. G. and C. A. Mead. Barrier height studies on metal-semiconductor systems. Journal of Applied Physics 34:3061-3069. 1963.

31. Texas Instruments, Incorporated. Second report for research and development of high temperature semiconductor devices. Dallas, Texas. July 1, 1959 through September 30, 1959. (Under contract no. NOBsr-77532(1734F).

32. Turner, D. R. and H. A. Sauer. Ohmic contacts to semiconductor ceramics. Journal of the Electrochemical Society 107:250-251. 1960.

APPENDIX

APPENDIX - PART I

Methods of applying contacts to N-type gallium arsenide found in the literature.

1. Evaporated Layers - 500 Å Sn and 5000 Å Ag - heat treatment at 500° in an inert atmosphere (17).
2. Alloyed pellets Au - Sn in various proportion - alloyed at temperatures between 500° and 600°C (17).
3. Pure tin alloyed at 450°C in forming gas (7).
4. Evaporate Au - Sn, Ni, and Au. Sinter at 400°C for 15 minutes (5).
5. Electroplate the GaAs with silver. Discharge a .25 uf capacitor between the contacts. Replate with silver (6).
6. Gold wires "formed" to the GaAs by a capacitor discharge (6).
7. Thermal-compression-bonded gold at 500°C (6).
8. Gold alloyed at 550-600°C (6;24).
9. GaAs bonded to antimony-gold plated Kovar at 450°C (20).
10. Alloy tin to freshly etched surface using lactic acid as a flux (1).
11. Electroless-nickel plating to the GaAs followed by tinning with lead-tin solder (32).
12. Vacuum deposit tin and nickel coatings. Heat in a vacuum furnace to a temperature at which the tin starts to diffuse. Solder (27).

13. Evaporate a 1.5 μ layer of 50 Au - 50 Sn. Alloy at 290°C. Evaporate another 0.5 μ layer of 50 Au - 50 Sn and nickel plate using electroless-nickel plating (5).

14. Alloy the GaAs to a gold-tin plated moly wire (4).

15. Alloy the GaAs with a silver-tin alloy (17).

16. Solder the GaAs to the holder using lead-tin solder (23).

17. Alloy indium to the GaAs at 500°C (21).

18. Alloy the GaAs with tin which has been doped with sulphur, germanium, or tellerium (13).

19. Evaporate tin on to a heated (200°C) wafer to GaAs. Electroplate with nickel and sinter at 600°C for 10 minutes. Electroplate with nickel followed by electroplating with gold (19).

APPENDIX - PART II

Method of applying contacts to P-type gallium arsenide found in the literature and by private communication.

1. Evaporate 500 Å Zn + 5000 Å Ag - Heat treat near 550°C. [1]
2. Evaporate silver onto GaAs held at 200°C. Then evaporate a layer of gold. [2]
3. Evaporate nickel followed by gold. Sinter in reducing atmosphere at 400°C for 15 minutes. [3]
4. Electroplate silver on the GaAs (2).
5. Gold wires "formed" to the GaAs by a capacitor discharge (6).
6. Thermal-compression-bonded gold at 500°C (6).
7. Alloy a 5 mil indium sphere at 250-300°C to the GaAs using a flux of aluminum chloride (20;24).
8. Displace gold on to the GaAs from a gold-chloride solution (1).
9. Electroless-nickel plating (32).
10. Evaporate and alloy a 0.3μ layer of indium (5).
11. Alloy 50 Au - 50 Zn to the GaAs (13).

---

[1] Archer, R. J., Staff Member Hewlett Packard Associates. Private Communication.

[2] Quist, Theodore M., Staff Member Lincoln Laboratories. Private Communication.

[3] Arnold, K., Staff Member General Telephone and Electronics Laboratories. Private Communication.

12. Au - Zn plated moly alloyed to the GaAs (17).

13. In, Pb-In, or Pb-In-Zn alloys alloyed to the GaAs (17).

14. Lead-zinc or indium-zinc alloyed to the GaAs (13;23).

15. Indium soldered to the GaAs in flowing argon (21).

16. Electroplate with nickel and gold (19).

17. Evaporate aluminum and alloy at 650^{o}C (18).

APPENDIX - PART III

Measurements on the Linear Methods of Making Contact

	R-ohms	ω_1 x 10 6/sec.	C-pf	1/R-mhos
Aluminum Lapped	3	785	425	0.333
	3.77	742	358	0.265
	5.07	660	300	0.197
	4.35	630	366	0.230
	3.15	942	338	0.318
	4.4	630	362	0.227
	3.18	942	334	0.315
Zinc Lapped	2.05	765	636	0.488
	2.05	973	500	0.488
	2	780	642	0.500
	1.92	755	690	0.520
	2.39	848	495	0.418
	1.59	880	716	0.630
	1.83	755	725	0.546
	1.83	785	696	0.546
Zinc Etched	0.35	1350	2120	0.286
	0.4	1320	1900	0.250

APPENDIX -PART IV

Measured Values of R_B for the Non-linear Contact.

Method	R_B-ohms
Silver	
Lapped	9.4
*Silver	
*Lapped	8.8
Nickel	
Lapped	9.1
	8
	9.8
	9
	9.3
Etched	8.8

*Heat treated

APPENDIX - PART V

Average Non-Linear Total Resistance in Ohms at ± 0.5 Volts for the Non-Linear Contacts.

*Silver

Etched	Lapped
1660	22
5000	33
1660	32
1080	37
1110	19
834	
1660	
1660	

Silver

Etched	Lapped
124	36
200	50
770	26
	21
	18
	33
	33
	35
	50
	50
	42

Nickel

Etched	Lapped
550	43
308	37
244	39
238	35
81	36
190	32
	28
	33
	31
	29
	28
	31
	32
	36
	38

Indium

Lapped and Etched
14.3K
5.9K
10. K
2.86K
2.63K
14.3K
3.33K

*Heat treated